The Canadian Mineralogist
Vol. 47, pp. 3-24 (2009)
DOI : 10.3749/canmin.47.1.3

THE CRYSTAL STRUCTURE OF SULFOSALTS WITH THE BOXWORK ARCHITECTURE AND THEIR NEW REPRESENTATIVE, $Pb_{15-2x}Sb_{14+2x}S_{36}O_x$

EMIL MAKOVICKY[§]

Department of Geography and Geology, University of Copenhagen, Østervoldgade 10, DK–1350 Copenhagen, Denmark

DAN TOPA

Department of Material Research & Physics, University of Salzburg, Hellbrunnerstrasse 34, A–5020 Salzburg, Austria

ABSTRACT

The new monoclinic phase with a structure-determined formula $Pb_{15-2x}Sb_{14+2x}S_{36}O_x$ (Z = 4) was found only as a single grain in a micro-intergrowth of sulfosalts in the Klačianka Sb deposit, Low Tatra Mountains, Slovakia. Unit-cell dimensions are *a* 48.293(15), *b* 4.1107(13), *c* 34.223(11) Å, β 106.168(5)°, space group *C*2/*m*. There are 11 independent lead sites, 13 antimony sites, and five mixed (Pb, Sb) sites, 36 sulfur positions, and a single, approximately half-occupied oxygen site. Some coordination polyhedra of antimony exhibit split Sb sites, with positional parameters refined independently. Because of the intergrowth, the final R_1 value remained at 23.5%. It does not reflect visibly upon positional parameters, but has an adverse influence on the occupancy of mixed positions. Until further occurrences are documented, it remains an unnamed mineral. It is a typical sulfosalt representative of the category of boxwork structures. Other structures of this category comprise pellouxite, marrucciite, vurroite, neyite, and several synthetic sulfosalts. Sulfosalts with a boxwork structure are formed by a combination of three types of structural modules: continuous walls with a complex structure of rod-layer type; these walls are interconnected by partitions, and the resulting boxlike channels are filled by another type of structure rods. In its entirety, this group demonstrates a number of types for each of these kinds of module. The "core" group of Pb–Sb sulfosalts, scainiite, pillaite, pellouxite, rouxelite, a synthetic Mn–Pb sulfosalt, and $Pb_{15-2x}Sb_{14+2x}S_{36}O_x$ described in this study, depend on the presence of minor amounts of oxygen in the structures. Oxygen forms a part of a kermesite-like configuration that generates a pronounced change of the local structural arrangement and, in this way, makes the boxwork framework possible. Several REE sulfides form boxwork structures as well.

Keywords: boxwork structures, sulfosalts, unnamed Pb–Sb oxysulfosalt, crystal structure, Klačianka deposit, Low Tatra Mountains, Slovakia.

SOMMAIRE

Un seul grain d'une nouvelle phase monoclinique ayant la formule $Pb_{15-2x}Sb_{14+2x}S_{36}O_x$ (Z = 4), telle que déterminée par affinement de la structure, a été découvert en micro-intercroissance de sulfosels dans un échantillon provenant du gisement d'antimoine de Klačianka, montagnes Basse Tatra, en Slovaquie. Les paramètres réticulaires sont: *a* 48.293(15), *b* 4.1107(13), *c* 34.223(11) Å, β 106.168(5)°, groupe spatial *C*2/*m*. Il y a 11 sites indépendants de plomb, 13 d'antimoine, et cinq à caractère mixte (Pb, Sb), 36 positions de soufre, et un seul site d'oxygène, environ à moitié occupé. Certains des polyèdres de coordinence de Sb font preuve d'un site Sb dédoublé, avec des paramètres positionnels affinés indépendemment. A cause de l'intercroissance, la valeur finale de R_1 est demeurée élevée, 23.5%. Ce résultat visiblement n'affecte pas les paramètres positionnels, mais exerce une influence adverse sur l'affinement des taux d'occupation des sites. En attendant la découverte d'autres exemples, cette phase demeurera un minéral sans nom. C'est un sulfosel typique de la catégorie des structures emboîtées. Font aussi partie de cette catégorie pellouxite, marrucciite, vurroïte, neyite, et plusieurs sulfosels synthétiques. Les sulfosels à structure emboîtée contiennent en combinaison trois types de modules: des parois continues avec une structure complexe de tiges en couches; ces parois sont interconnectées par des partitions, et les canaux ressemblant à des boîtes sont remplis d'une autre sorte de tiges structurales. Dans l'ensemble, ce groupe démontre plusieurs variantes pour chaque sorte de module. Le groupe "central" de sulfosels Pb–Sb, soient scainiite, pillaïte, pellouxite, rouxelite, un sulfosel synthétique contenant Mn–Pb, et $Pb_{15-2x}Sb_{14+2x}S_{36}O_x$ décrit dans ce travail, dépendent de la présence de faibles quantités d'oxygène incorporées dans la structure. Les atomes d'oxygène font partie d'une configuration semblable à la kermesite, qui mène à un changement prononcé dans l'agencement local dans la structure et, ainsi, rend possible la charpente emboîtée. Plusieurs sulfures de terres rares forment de telles structures.

(Traduit par la Rédaction)

Mots-clés: structures emboîtées, sulfosels, oxysulfosel Pb–Sb sans nom, structure cristalline, gisement de Klačianka, montagnes Basse Tatra, Slovaquie.

[§] *E-mail address*: emilm@geol.ku.dk

INTRODUCTION

Since the solution of the crystal structure of Sb_2S_3 by Hofmann (1933), which clarified the coordination properties of Sb^{3+}, the complexity of sulfosalt structures treated has been growing steadily. Examples of stepping stones on this path are jamesonite (Niizeki & Buerger 1957), robinsonite (Petrova *et al.* 1978) and kobellite (Miehe1971). The challenge of solving the structure of izoklakeite, a member of the kobellite–izoklakeite family (Makovicky & Mumme 1986) has been superseded in 2000–2001 by structure determinations on scainiite, $Pb_{14}Sb_{30}S_{54}O_5$ (Moëlo *et al.* 2000), neyite $Ag_2Cu_6Pb_{25}Bi_{26}S_{68}$ (Makovicky *et al.* 2001) and pillaite (Meerschaut *et al.* 2001). Makovicky *et al.* (2001) introduced the name of *boxwork structures* to refer to their architecture. The number of boxwork structures of sulfosalts published is growing every year, as is also the variety of principles involved in their construction. A literature search revealed analogous structures among synthetic sulfosalts, *e.g.*, $In_4Bi_2S_9$ (Chapuis *et al.* 1972) and rare-earth sulfides.

The structures of this category can be understood as an extension of the principle of rod-based structures (rod layers, rod chessboards, *etc.*), which was worked out by Makovicky (1993, 1997) for less complex families of sulfosalts and then applied to a number of new structures. This principle was also applied to several Pb–Sb–S–O sulfosalts (such as scainiite and pillaite) by the Nantes – Pisa research group but, starting with their study of scainiite, they favored an alternative approach to modular analysis of the Pb–Sb sulfosalts that is based primarily on the kinship with cyclically twinned sulfosalt structures. Spurred by a discovery of a new Pb–Sb sulfosalt, $Pb_{15-2x}Sb_{14+2x}S_{36}O_x$, the boxwork structure of which is documented here, we have summarized the boxwork structures known today and made some generalizations that can be obtained *by considering the boxwork approach*, including the observations presented by the Nantes–Pisa group. We expect that the conclusions obtainable *by the cyclic approach* (see listing in Moëlo *et al.* 2008) will one day complete the understanding of the dual nature of this group. Our boxwork approach also differs from the approach of “couches gaufrées” (or palisade-like layers) developed by Moëlo *et al.* (2000) and Doussier *et al.* (2007), respectively, and discussed in more detail below.

THE OCCURRENCE OF $PB_{15-2X}SB_{14+2X}S_{36}O_X$

The material examined comes from the abandoned dumps of a small sulfide deposit of Klačianka in the old antimony mining region on the northern slopes of the Low Tatra Mountains, Slovakia. A single fragment of quartz matrix with aggregates of needle-like sulfosalt crystals yielded crystals of boulangerite, jamesonite, dadsonite and the hitherto unknown sulfosalt. We found it as a single tiny grain with domains in two orientations and in intimate intergrowth with other phases, while looking for a suitable crystal of dadsonite (Makovicky *et al.* 2006). Fundamental features of the new crystal structure were determined in 2003. Since then, neither examination of concentrates nor electron-microprobe examination of the material collected in Klačianka gave an indication of more material of the same kind. Therefore, the structure determination was carried out to its possible limits and the results are presented here.

EXPERIMENTAL DATA

Experimental and crystal data are presented in Table 1. Reflections of the reciprocal lattice of the new compound were separated as much as possible from those of the admixtures, but still the principal problem encountered with the structure determination stems from the numerous random overlaps with the reflections of minor phases present. In the final stage of refine-

TABLE 1. SINGLE-CRYSTAL X-RAY-DIFFRACTION: EXPERIMENTAL AND REFINEMENT DETAILS

Crystal data	
Chemical formula	$Pb_{51.8}Sb_{64.2}S_{114}O_{2.4}$
Chemical formula weight	23224.6
Cell setting, space group	monoclinic, *C2/m*
Unit-cell parameters	
a (Å)	48.293(15)
b (Å)	4.1107(13)
c (Å)	34.223(11)
α (°)	90.00
β (°)	106.168(5)
γ (°)	90.00
V (Å^3)	6525(4)
Z	1
D_x (Mg m^{-3})	5.91
No. of reflections for cell parameters	954
μ (mm^{-1})	40.6
Crystal form	needle-like
Crystal size (mm)	0.02 × 0.03 × 0.15
Crystal color	grey metallic
Data collection	
T_{min}, T_{max}	0.185, 0.426
No. of measured reflections	43192
No. of independent reflections	8929
No. of observed reflections	6318
Criterion for observed reflections	$I > 2\sigma(I)$
R_{int} (%)	18.6
θ_{max} (°)	28.3
Range of *h*, *k*, *l*	$-63 \le h \le 63$, $-5 \le k \le 5$, $-44 \le l \le 44$
Refinement	
Refinement on F_o^2, $R[F_o > 4\sigma(F_o)]$ (%)	23.35
$wR(F_o^2)$ (%)	25.89
S (GooF)	1.969
No. of reflections used in refinement	6318
No. of parameters refined	393
Weighting scheme $w = 1/[\sigma^2(F_o^2)+(aP)^2+bP]$, where $P = (F_o^2 + 2F_c^2) / 3$	a = 0.2, b = 0
$(\Delta/\sigma)_{max}$	0.01
$\Delta\rho_{max}$ (e/Å^3)	18.81 (0.43 Å from Pb4)
$\Delta\rho_{min}$ (e/Å^3)	−7.95 (1.44 Å from S14)
Extinction coefficient	0.0047(4)
Source of atomic scattering factors: *International Tables for X-Ray Crystallography* (1992, Vol. C, Tables 4.2.6.8 and 6.1.1.4)	
Computer programs	
Structure solution	SHELXS 97 (Sheldrick 1997a)
Structure refinement	SHELXL 97 (Sheldrick 1997b)

ment, fifty manifestly wrong intensities were rejected, but many reflections still suffer from non-removable overlaps, arresting the R_1 value of an obviously right structure solution at 23.5%. The current sulfosalt is not the only boxwork structure with high R values; for example, marrucciite (Orlandi *et al.* 2007) has R_1 equal to 9.6%, and in rouxelite (Orlandi *et al.* 2005), R_1 is equal to 16.9% because of the quality of the material available.

Although no reflections suggesting a doubled (~8 Å) periodicity were found or proven, the structure contains several mixed (Sb,Pb) sites, a partially occupied site of oxygen, and at least one site, Sb16, that displays anisotropic displacement parameters suggestive of a split above and below the mirror planes of the space group *C*2/*m* selected for the structure determination. A part of the light atoms (sulfur) had to be refined with isotropic displacement parameters. The inferior quality of the intensity data reflects unfavorably upon the site occupancies of cations in the mixed sites and occupancy of the oxygen position. The former occupancies have standard errors at about 10% of the occupancy values, the occupancy of the O site was refined as 0.59(17), with $\sigma(U_{iso})$ found to be large as well. Fluctuation of occupancy of the mixed sites in different cycles of least-squares refinement is of the order of 1–2 σ, whereas their positional coordinate values, and those of all other cations and sulfur atoms, vary insignificantly, within the limits of their low σ values. In terms of electrons *per site*, the differences between different results for the occupancy of the oxygen position are minute, compared to the Z values of Pb and Sb. Tables 2 and 3 contain the structural information, whereas a comparison with other related phases is made in Table 4.

DESCRIPTION OF COORDINATION POLYHEDRA IN $Pb_{15-2x}Sb_{14+2x}S_{36}O_x$

The crystal structure of $Pb_{15-2x}Sb_{14+2x}S_{36}O_x$ contains eleven independent pure lead sites, 13 coordination polyhedra of antimony, some of them with split Sb sites, and five mixed Pb,Sb sites. This results in the ideal formula $M_{29}S_{36}O_x$ (Z = 4), where *x* is the empirical oxygen content, theoretically from nil to a full O site *pfu*. The results of the refinement, with limitations imposed upon calculated occupancies by the inferior quality of diffraction data to be considered, result in the empirical formula $Pb_{51.8}Sb_{64.2}S_{144}O_{2.4}$, which has unbalanced valences and differs from the formula $Pb_{55.2}Sb_{60.8}S_{144}O_{2.4}$, calculated for the sulfur and oxygen contents as refined. Calculations with no oxygen present result in a theoretical formula $Pb_{60}Sb_{56}S_{144}$, whereas those with a full oxygen site yield $Pb_{52}Sb_{64}S_{144}O_4$. Thus, the *general formula* is $Pb_{60-2x}Sb_{56+2x}S_{144}O_x$, which can be simplified to $Pb_{15-2x}Sb_{14+2x}S_{36}O_x$, Z = 4, the formula used in this paper.

The coordination polyhedra of lead are mono- and bicapped trigonal coordination prisms, positioned typically on the outer surfaces of Pb–Sb rods (*i.e.*, acting as envelopes of lone-electron-pair micelles of Sb); they are intermeshed with the coordination pyramids of antimony, which are concentrated in the rod interior. Eight of them are "standing prisms" with the (approximate) three-fold axes parallel to the rods (*i.e.*, *b* axis), and three are "lying-down prisms" with three-fold axes at 90° to the rod elongation. A three-fold group of bicapped coordination prisms, Pb2–Pb4–Pb5, and the only tricapped trigonal prismatic Pb site, Pb 7, respectively, bind together three adjacent rods (micelles) at two different points of the structure. The Pb–S distances are recorded in Table 3.

The coordination polyhedra of antimony are square coordination pyramids completed by two additional S atoms under the base to monocapped trigonal prisms. The Sb atom is situated in the prism wall, and the lone electron-pair of Sb, in the volume of the prism. The distance of the additional S from Sb may exceed 4 Å, but the shape of the prism is only rarely distorted: this happens for Sb8 and Sb11 by a partial closure of the lone-electron-pair micelle, and especially for Sb10, which faces the Sb14 site (Figs. 1, 2). The Sb14 atom is bound to oxygen and has an entirely reorganized scheme of Sb–S bonds. An even distribution between "standing" and "lying-down" coordination prisms of Sb is observed.

Two basic schemes of bonding are recognized for antimony: the 3 + 2 + 2 scheme of asymmetrically coordinated Sb atoms, and the 1 + 4 + 2 scheme for Sb pyramids situated centrally in the *3- and 4-fold ribbons* of Sb coordination pyramids, which can be traced out in the structure. Anisotropic displacement parameters and the empirical bond-lengths indicate that the latter type of coordination consists of two split "half-atoms" biased asymmetrically each to its side of a pyramid, as observed, *e.g.*, in boulangerite (Mumme 1989) and dadsonite (Makovicky *et al.* 2006). The position Sb18,19 in the central portions of the lone-electron-pair micelle outlined by Sb5–Sb15, and the position Sb6,7 in the environment saturated with mixed Pb,Sb sites, were split successfully during the refinement, whereas a similar indication for Sb9 did not result in a split site. In the cases like Sb9, we see a weighted average of two cation positions and a corresponding average of bond lengths to the sulfur ligands (Makovicky *et al.* 2006). For the split cation-positions, the exact positions of the ligands at the vertices of the polyhedron differ somewhat for the two cation positions, and the anions refined represent unresolved weighted averages of these anion sites. In both cases, the resulting apparent bond-distances are affected, although to a different degree (Berlepsch *et al.* 2001, Makovicky *et al.* 2006).

As already stated, anisotropic displacement parameters indicate that Sb16 and, to a lesser degree, also

TABLE 2. POSITIONAL AND ATOMIC DISPLACEMENT PARAMETERS FOR $Pb_{15-2x}Sb_{14+2x}S_{36}O_x$

Atom	sof	x	y	z	U_{eq}	U_{11}	U_{22}	U_{33}	U_{13}
Pb1	0.59(5)	0.0228(5)	0.5	0.1648(6)	0.041(4)	0.042(9)	0.038(5)	0.051(7)	0.029(7)
Sb1	0.41(5)	0.013(1)	0.5	0.1579(19)	0.046(9)	0.031(16)	0.045(14)	0.076(25)	0.036(18)
Pb2		0.0443(1)	0	0.3828(2)	0.041(1)	0.027(2)	0.027(2)	0.071(3)	0.017(2)
Pb3	0.78(5)	0.0865(2)	0.5	0.0997(3)	0.037(2)				
Sb2	0.22(5)	0.0855(10)	0.5	0.0886(23)	0.041(12)				
Pb4		0.1127(1)	0	0.3191(1)	0.036(1)	0.046(2)	0.024(2)	0.039(2)	0.011(2)
Pb5		0.1355(1)	0	0.4541(1)	0.034(1)	0.036(2)	0.020(2)	0.039(2)	-0.002(2)
Pb6		0.1698(1)	0	0.1191(1)	0.038(1)	0.035(2)	0.032(2)	0.040(2)	0.001(2)
Pb7		0.1756(1)	0	0.2454(2)	0.051(1)	0.060(3)	0.031(2)	0.062(3)	0.018(2)
Pb8		0.2849(1)	0.5	0.2961(1)	0.042(1)	0.058(3)	0.028(2)	0.036(2)	0.010(2)
Pb9		0.3248(1)	0.5	0.4209(1)	0.028(1)	0.032(2)	0.019(2)	0.032(2)	0.006(1)
Pb10		0.3490(1)	0.5	0.0110(1)	0.039(1)	0.042(2)	0.034(2)	0.039(2)	0.010(2)
Pb11		0.3645(1)	0.5	0.1446(2)	0.042(1)	0.049(2)	0.030(2)	0.058(3)	0.032(2)
Pb12		0.3684(1)	0.5	0.2751(2)	0.060(2)	0.065(3)	0.030(2)	0.069(3)	-0.009(3)
Pb13		0.4551(1)	0.5	0.3331(1)	0.029(1)	0.028(2)	0.022(2)	0.035(2)	0.006(1)
Sb3	0.89(4)	0.0073(2)	0	0.0537(3)	0.065(3)	0.049(5)	0.108(8)	0.045(5)	0.027(4)
Pb14	0.11(4)	0.0073(2)	0	0.0537(3)	0.065(3)	0.049(5)	0.108(8)	0.045(5)	0.027(4)
Sb4		0.0326(2)	0.5	0.2693(3)	0.05(2)	0.066(5)	0.035(4)	0.041(4)	-0.007(4)
Sb5		0.0753(2)	0.5	0.5034(2)	0.042(2)	0.035(3)	0.057(5)	0.043(4)	0.024(3)
Sb6	0.55(4)	0.1033(4)	0.5	0.2000(5)	0.044(5)				
Sb7	0.45(4)	0.0917(4)	0.5	0.2087(5)	0.034(6)				
Sb8		0.1863(1)	0.5	0.3860(2)	0.031(2)	0.028(3)	0.027(3)	0.045(4)	0.019(3)
Sb9		0.2237(2)	0.5	0.0589(3)	0.053(2)	0.041(4)	0.013(3)	0.106(7)	0.020(4)
Sb10		0.2402(2)	0.5	0.1859(2)	0.043(2)	0.041(4)	0.028(3)	0.045(4)	-0.012(3)
Sb11		0.2447(2)	0	0.3659(3)	0.050(2)	0.067(5)	0.033(4)	0.064(5)	0.043(5)
Sb12		0.2830(2)	0	0.4924(3)	0.037(2)	0.038(3)	0.020(3)	0.066(5)	0.034(4)
Sb13		0.2931(2)	0	0.0692(3)	0.039(2)	0.031(3)	0.021(3)	0.067(5)	0.014(3)
Sb14		0.3075(2)	0	0.1991(2)	0.042(2)	0.023(3)	0.060(5)	0.042(4)	0.008(3)
Sb15		0.3973(2)	0	0.3861(2)	0.043(2)	0.054(4)	0.045(4)	0.037(4)	0.025(3)
Sb16		0.4294(2)	0.5	0.0094(5)	0.077(4)	0.037(4)	0.153(11)	0.041(5)	0.013(4)
Pb15	0.50(5)	0.4404(3)	0.5	0.1103(5)	0.037(4)				
Sb17	0.50(5)	0.4429(5)	0.5	0.1194(9)	0.040(7)				
Sb18	0.32(14)	0.4915(9)	0	0.4481(14)	0.014(11)				
Sb19	0.64(14)	0.4852(9)	0	0.4396(12)	0.040(4)				
Sb20	0.47(5)	0.4522(2)	0	0.2229(2)	0.051(2)	0.083(5)	0.033(3)	0.052(4)	0.040(3)
Pb16	0.53(5)	0.4522(2)	0	0.2229(2)	0.051(2)	0.083(5)	0.033(3)	0.052(4)	0.040(3)
S1		0.0082(8)	0	0.2933(8)	0.047(8)	0.091(24)	0.013(10)	0.032(13)	0.007(14)
S2		0.0402(5)	0.5	0.0295(8)	0.037(6)	0.013(9)	0.038(13)	0.044(14)	-0.020(9)
S3		0.0457(4)	0	0.1203(9)	0.031(6)	0.007(7)	0.016(9)	0.073(17)	0.014(9)
S4		0.0687(7)	0	0.2351(9)	0.061(9)	0.055(18)	0.105(29)	0.036(15)	0.036(14)
S5		0.0694(6)	0.5	0.3329(7)	0.029(5)	0.049(14)	0.016(9)	0.025(10)	0.015(10)
S6		0.0840(5)	0.5	0.4343(5)	0.021(5)	0.040(11)	0.025(10)	0.001(7)	0.010(7)
S7		0.1116(6)	0	0.5267(8)	0.038(6)				
S8		0.1270(5)	0	0.1746(9)	0.040(6)	0.021(10)	0.053(16)	0.049(15)	0.014(10)
S9		0.1365(4)	0.5	0.3889(6)	0.023(5)	0.017(8)	0.002(7)	0.033(11)	-0.020(8)
S10		0.1381(7)	0.5	0.2654(9)	0.046(7)	0.062(18)	0.035(14)	0.036(14)	0.004(14)
S11		0.1725(7)	0.5	0.0550(7)	0.039(7)	0.093(22)	0.015(10)	0.013(10)	0.024(11)
S12		0.1780(9)	0	0.3350(16)	0.086(15)	0.117(36)	0.062(23)	0.115(36)	0.095(33)
S13		0.1903(8)	0.5	0.1826(9)	0.046(8)	0.090(22)	0.008(9)	0.065(18)	0.065(18)
S14		0.2139(7)	0	-0.0004(9)	0.055(9)	0.046(16)	0.063(20)	0.036(14)	-0.022(12)
S15		0.2288(72)	0	0.1206(10)	0.060(10)	0.053(18)	0.046(17)	0.051(17)	-0.035(15)
S16		0.2306(9)	0.5	0.3133(13)	0.067(10)				
S17		0.2464(6)	0	0.2376(8)	0.043(7)	0.030(12)	0.073(20)	0.033(13)	0.020(10)
S18		0.2691(7)	0.5	0.4349(9)	0.047(7)				
S19		0.2952(5)	0	0.3588(6)	0.021(4)	0.028(10)	0.025(10)	0.010(8)	0.003(7)
S20		0.3001(7)	0.5	0.5499(9)	0.051(8)	0.031(13)	0.064(20)	0.053(17)	0.004(12)
S21		0.3023(9)	0.5	0.1233(8)	0.066(11)	0.128(35)	0.052(19)	0.014(11)	0.0144(16)
S22		0.3241(6)	0	0.2751(8)	0.043(7)	0.050(16)	0.035(13)	0.030(12)	-0.013(11)
S23		0.3320(4)	0	0.4844(8)	0.024(5)	0.010(8)	0.004(7)	0.057(14)	0.006(8)
S24		0.3445(5)	0	0.0729(8)	0.028(5)	0.027(10)	0.011(9)	0.056(15)	0.030(11)
S25		0.3581(5)	0	0.2000(8)	0.029(5)	0.030(11)	0.014(9)	0.044(13)	0.011(10)
S26		0.3627(6)	0.5	0.3589(8)	0.035(5)				
S27		0.3911(2)	0.5	-0.0580(8)	0.037(6)	0.028(11)	0.051(16)	0.033(12)	0.009(10)
S28		0.4013(11)	0	0.0356(16)	0.087(13)				
S29		0.4107(4)	0	0.3206(8)	0.031(6)	0.008(8)	0.026(11)	0.043(13)	-0.022(8)
S30		0.4175(5)	0	0.1472(7)	0.027(4)	0.028(10)	0.030(11)	0.026(11)	0.013(9)
S31		0.4222(4)	0.5	0.2348(9)	0.033(6)	0.005(7)	0.017(9)	0.064(16)	-0.0142(9)
S32		0.4444(5)	0.5	0.4139(6)	0.029(5)	0.033(1)	0.050(14)	0.005(8)	0.006(8)
S33		0.4795(6)	0	0.0893(7)	0.031(5)	0.044(13)	0.033(12)	0.023(11)	0.020(10)
S34		0.4857(5)	0.5	0.1787(7)	0.025(4)				
S35		0.4991(8)	0	0.3757(8)	0.056(10)	0.084(22)	0.016(11)	0.034(13)	-0.040(14)
S36		0.5281(5)	0.5	0.4679(11)	0.062(10)	0.013(10)	0.092(27)	0.076(23)	0.005(12)
O	0.59(9)	0.3068(21)	0.5	0.2154(30)	0.023(30)				

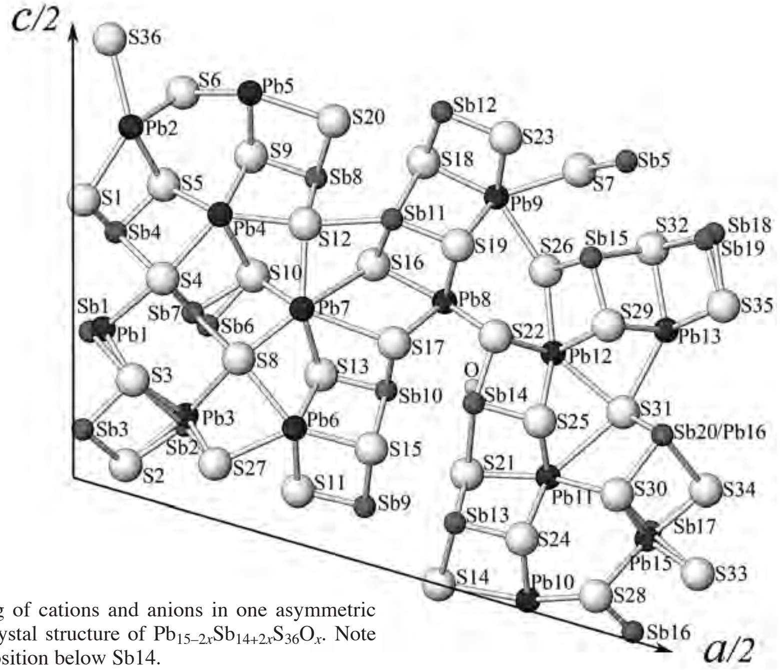

FIG. 1. Labeling of cations and anions in one asymmetric unit of the crystal structure of $Pb_{15-2x}Sb_{14+2x}S_{36}O_x$. Note the oxygen position below Sb14.

Sb14 and Sb5, might be positions split along the 4 Å *b* axis. In the case of Sb14, this might be connected with bond formation to oxygen because, with a lack of visible superstructure, Sb14 might be bonding randomly to the ligand below, or above, its level. The bond-length scheme (Table 3) suggests a similar disorder along the *b* direction for Sb19 as well.

The mixed sites are concentrated in a rod of SnS-like structure, which fills the box-like void of the boxwork structure (Fig. 2). Three such sites, Sb1–Pb1, Sb2–Pb3 and Sb17–Pb15, were refined as split sites, with every fractional atom having its own coordinates and a label. Two more sites, Sb3 and Sb20, could only be refined as unsplit sites in which Sb and Pb have the same set of coordinates. In all cases, complete occupancy of a coordination polyhedron was assumed. The Pb atoms protrude from the base of the pyramid and, for well-split cases, the relevant bond-distances approximate those of pure Pb and Sb (not forgetting, however, that their ligands represent mixed positions in such a case). All mixed sites form standing, monocapped trigonal coordination prisms.

The Sb14 site is a specific antimony site of decisive importance for oxysulfosalts of Pb and Sb (Moëlo *et al.* 2000). The three nearly perpendicular short Sb–anion bonds are: (1) Sb14–S25 (2.464 Å) to the vertex of the configuration, which remained from the "reduction" of the coordination pyramid SbS_5, analogous to those of the Sb neighbors, (2) Sb14–S22 (2.499 Å) to a new S position with the same *y* height as Sb14, and (3) S14–O (2.128 Å), which is oriented along +*y* or –*y* with equal probability. Two additional distances, Sb14–S21, are 3.264 Å. The Sb–O distance is an average distance because both Sb14 and O display a pronounced (oriented) displacement parallel to [010]. The half-occupied O site suggests that each Sb14 atom has only one oxygen neighbor. Doussier *et al.* (2007) modeled this coordination as a mean of 2.02 Å for the Sb–O bond and 2.36 Å for the Sb–vacancy distance; these differences are obtained by displacements of Sb toward oxygen and away from vacant sites, similar to our displacements. Doussier *et al.* (2007) assumed a half-filled oxygen site in the synthetic Mn sulfosalt they studied, similar to our direct refinement results. The oxygen positions in scainiite (Moëlo *et al.* 2000) were refined as two full and one half-occupied site, in pillaite (Meerschaut *et al.* 2001) and pellouxite (Palvadeau *et al.* 2004) as a half-occupied site, and in rouxelite (Orlandi *et al.* 2005) as a ~2/3 occupied position.

MODULAR DESCRIPTION AND AFFINITIES

A modular description of $Pb_{15-2x}Sb_{14+2x}S_{36}O_x$ requires a prior definition of what is a boxwork structure (configuration), what are the individual module categories involved, and what are their mutual relationships.

Boxwork structures: definition and architecture

Boxwork structures are the most complex modular category of structures of sulfosalts and other complex sulfides known to date. Their name (Makovicky *et al.* 2001) comes from the arrangement of structural elements into a *framework* of *walls* interconnected by *partitions*, which together delimit large *quadrilateral channels* filled by structural elements that are crystal-chemically similar to, although not identical with, the elements that constitute the channel walls. The boxwork structures thus are not a category of micro- or mesoporous structures, in which the *channel fill* is profoundly different from the structure framework and even may be exchanged under certain conditions (Makovicky 2005).

This definition allows for a variety of principles in wall and partition construction as well as in the box fill, but the majority of sulfosalt structures known to date, those determined chiefly by the members of the Nantes–Pisa research group, follow a rather narrow set of principles, making possible a unified description of this "principal" Pb–Sb subgroup of (primarily) oxysulfosalts. The "aberrant" cases can generally be interpreted as related to definite groups of sulfosalts lying outside the boxwork category. Prominent cases of boxwork structures also exist among the chalcogenides of rare-earth elements.

As already mentioned, the category of boxwork structures overlaps partly with another large category of complex sulfides, the *derivatives of the cyclically twinned structures,* known among sulfosalts and other complex sulfides (Moëlo *et al.* 2000, 2008). Thus, several important boxwork sulfosalts, *e.g.*, pillaite, scainiite and the present sulfosalt, can be described with equal validity as structures derived from cyclically twinned sulfosalt structures of zinckenite or barium–bismuth sulfide type (Makovicky 1985); they were

TABLE 3. BOND DISTANCES (Å) IN POLYHEDRA IN $Pb_{15-2x}Sb_{14+2x}S_{36}O_x$

Pb1-	Sb1-	Pb2-	Pb3-	Sb2-	Pb4-	Pb5-
S33 2.835(29)	S33 2.447(58)	S35 2.961(28)×2	S2 2.789(23)	S2 2.540(54)	S12 3.050(53)	S7 3.018(31)
S34 2.852(25)×2	S34 2.636(42)×2	S6 3.021(14)×2	S27 2.879(22)×2	S27 2.701(47)×2	S5 3.059(23)×2	S9 3.044(18)×2
S3 2.950(28)×2	S3 3.092(52)×2	S1 3.073(26)	S3 3.062(20)×2	S3 3.196(52)×2	S4 3.061(28)	S23 3.045(16)×2
S4 3.458(27)×2	S4 3.813(47)×2	S5 3.125(23)×2	S8 3.439(21)×2	S8 3.681(51)×2	S9 3.118(16)×2	S20 3.149(31)
		S36 3.219(42)			S10 3.221(28)×2	S6 3.153(18)×2
Pb6-	Pb7-	Pb8-	Pb9-	Pb10-	Pb11-	Pb12-
S15 2.829(35)	S8 2.865(24)	S16 2.845(48)	S18 2.868(37)	S14 2.957(34)	S25 2.871(21)×2	S26 2.952(30)
S13 2.955(23)×2	S10 2.941(26)×2	S19 2.912(15)×2	S23 2.941(20)×2	S24 3.004(21)×2	S21 2.887(47)	S22 2.966(22)×2
S11 3.034(18)×2	S12 3.035(57)	S22 3.012(23)×2	S19 3.016(14)×2	S11 3.015(14)×2	S24 3.141(20)×2	S29 3.009(14)×2
S27 3.098(22)	S13 3.195(30)×2	S17 3.102(18)×2	S7 3.094(26)	S28 3.183(38)×2	S30 3.261(20)×2	O 3.102(85)
S8 3.175(32)	S17 3.506(31)	O 3.238(**)	S26 3.165(32)	S27 3.518(30)	S31 3.535(23)	S25 3.219(21)×2
	S16 3.640(31)×2	S26 3.771(26)				S31 3.264(27)
Pb13-	Sb3/Pb14-	Sb4-	Sb5-	Sb6-	Sb7-	Sb8-
S29 2.916(14)×2	S3 2.507(24)	S5 2.396(24)	S6 2.515(21)	S10 2.396(31)	S10 2.523(32)	S9 2.434(22)
S32 2.951(23)	S2 2.859(21)×2	S1 2.613(25)×2	S7 2.675(17)×2	S8 2.616(23)×2	S4 2.614(26)×2	S12 2.654(34)×2
S35 3.019(23)×2	S33 2.901(22)×2	S4 3.126(29)×2	S36 3.058(18)×2	S4 3.095(32)×2	S8 3.098(28)×2	S20 2.944(24)×2
S1 3.220(40)	S2 3.735(20)×2	S34 3.880(19)×2	S32 3.826(21)×2	S3 3.896(23)×2	S3 3.817(24)×2	S16 3.706(50)
S31 3.297(28)						S18 3.878(32)
Sb9-	Sb10-	Sb11-	Sb12-	Sb13-	Sb14-	Sb15-
S11 2.437(35)	S13 2.379(40)	S19 2.517(27)	S23 2.459(23)	S24 2.452(26)	O 2.128(28)×2	S29 2.496(29)
S14 2.834(22)×2	S17 2.674(18)×2	S16 2.692(27)×2	S18 2.795(23)×2	S21 2.719(19)×2	S25 2.430(26)	S26 2.650(17)×2
S15 2.908(25)×2	S15 2.973(24)×2	S12 3.098(51)	S20 2.806(22)×2	S14 3.073(24)×2	S22 2.499(27)	S32 3.016(17)×2
S21 3.823(42)	O 3.102(92)	S18 3.104(24)×2	S20 3.867(28)	S14 3.901(30)	S21 3.264(23)×2	S7 3.749(26)×2
S14 4.057(38)	S21 4.144(47)	S20 4.057(38)	S18 3.995(40)	S15 3.975(39)	S17 3.551(33)	
					S15 4.001(30)	
Sb16-	Pb15-	Sb17-	Sb18-	Sb19-	Sb20/Pb16-	
S27 2.522(24)	S34 2.723(25)	S34 2.461(31)	S35 2.602(60)	S35 2.457(56)	S31 2.611(16)×2	
S28 2.746(41)×2	S30 2.799(22)×2	S30 2.702(27)×2	S36 2.672(32)×2	S32 2.813(31)×2	S30 2.665(22)	
S2 3.041(23)×2	S33 3.010(26)×2	S33 3.070(32)×2	S32 3.047(36)×2	S36 2.887(32)×2	S34 3.239(22)×2	
S33 3.725(20)×2	S28 3.411(39)×2	S28 3.644(44)×2	S36 3.860(57)×2	S36 3.974(52)×2	S1 3.705(25)×2	

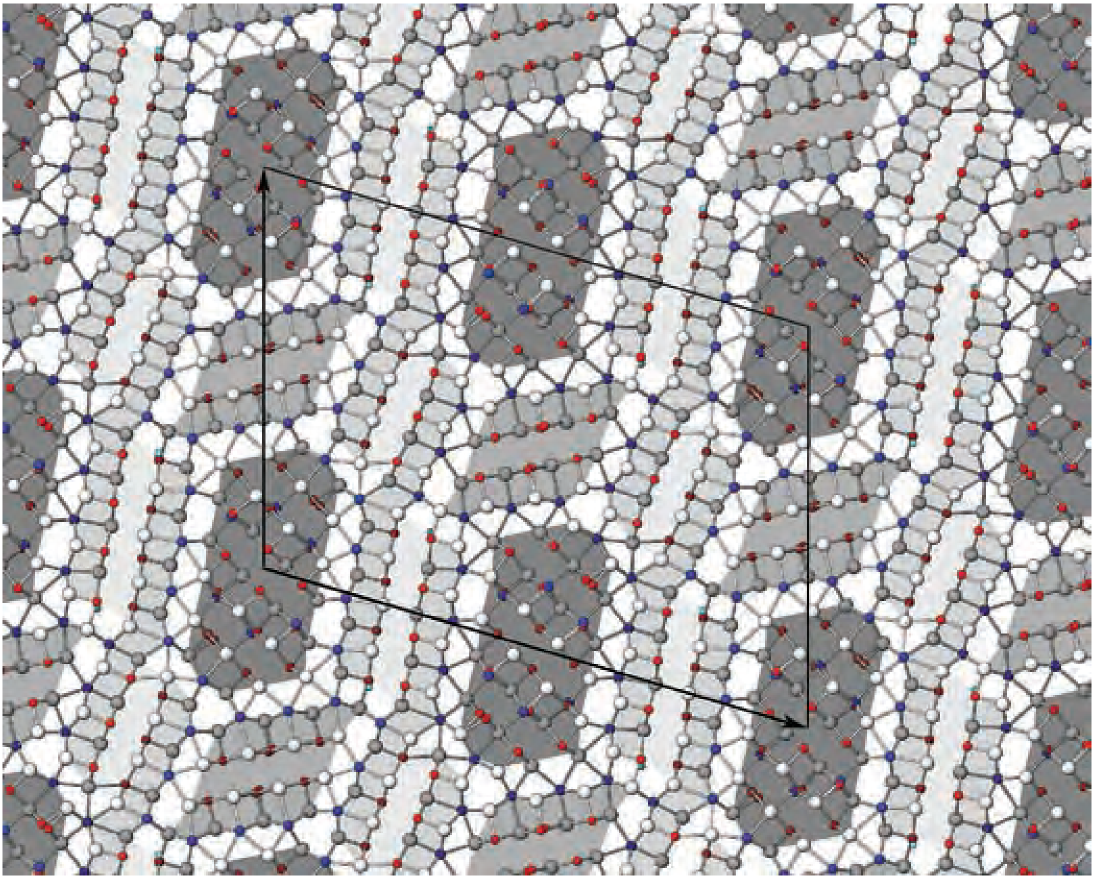

FIG. 2. The crystal structure of $Pb_{15-2x}Sb_{14+2x}S_{36}O_x$. Here and in the remaining figures, Pb is dark blue, Sb red, Hg, Ag or Mn (where applicable) are green, S and Bi are colorless, O is light blue, and Cl is yellow. Two kinds of rods forming walls (vertical in the figure) and their lone-electron-pair micelles (lighter, along median planes), and those forming partitions (horizontal) and boxwork fill, respectively, are delineated by increasingly dark shading. Non-commensurate interspaces between rods are left unshaded. Note the (capped) standing and lying-down trigonal coordination prisms of Pb.

classified as such by Moëlo *et al.* (2008). The duality of description is the best expression of the dual nature of these structures. However, not all important cases of the boxwork category are "cyclic derivatives", *e.g.*, neyite (Makovicky *et al.* 2001) and $La_{10}Er_9S_{27}$ (Carré & Laruelle 1973, Makovicky 1992), whereas structures like $(Mn_{1-x}Pb_x)Pb_{10-y}Sb_{12-y}S_{26-y}Cl_{4+y}O$ (Doussier *et al.* 2007) are a boundary case. Besides the boxwork structures, *the derivatives of cyclically twinned structures* encompass other important groups of sulfosalts, such as the kobellite-type structures in the broadest sense. Treatment of the cyclic aspect of complex sulfosalts will not be taken up here, except for a short mention of its application to our new compound.

The structural elements of boxwork structures

The continuous *walls* in "typical" boxwork structures (drawn vertically in all figures) can be based on the SnS archetype, in a smaller number of cases on the PbS archetype or, being just a double layer, the archetype remains ambiguous (Makovicky 1997). In most cases, they represent an alternation of two types or rods along the layer. They are interconnected by a double layer $(100)_{SnS}$; this layer-building principle corresponds in principle to "Layer Type 1" observed in boulangerite (Makovicky 1993). In neyite, based on the PbS principle, the interconnection proceeds *via* a triple layer $(100)_{PbS}$.

TABLE 4. BOXWORK STRUCTURES AND RELATED PHASES

		Formula	*a* (Å)	*b* (Å)	*c* (Å)	β (°)	Z	S.G.	Vol. ($Å^3$)/ No.atoms	Ref.
1	unnamed	$Pb_{15-2x}Sb_{14+2x}S_{36}O_x$ (1)	48.293(15)	4.1107(13)	34.223(11)	106.168(5)	4	*C*2/*m*	6525/264	1
2	pellouxite	$Cu_{0.68}Ag_{0.26}Pb_{10.44}Sb_{11.56}S_{27.5}O_{0.5}Cl_{0.5}$	55.824(11)	4.0892(8)	24.128(5)	113.14(3)	4	*C*2/*m*	5065/202	2
3	pillaite	$Pb_9Sb_{10}S_{23}ClO_{0.5}$	49.490(10)	4.1259(8)	21.828(4)	99.62(3)	4	*C*2/*m*	4394/174	3
4	rouxelite	$Cu_2HgPb_{22}Sb_{28}S_{64}(O,S)_2$	43.113(9)	4.0591(8)	37.874(8)	117.35(3)	2	*C*2/*m*	5887/238	4
5	marruccite	$Hg_3Pb_{16}Sb_{18}S_{46}$	48.320(10)	4.117(1)	24.056(5)	118.84(3)	2	*C*2/*m*	4193/166	5
6	scainiite	$Pb_{14}Sb_{30}S_{54}O_5$	51.996(8)	8.148(1)	24.311(4)	104.09(1)	4	*C*2/*m*	9990/412	6
7	synthetic	$Mn_{0.7}Pb_{11}Sb_{11.3}S_{25.3}Cl_{4.7}O$	37.480(8)	4.1178(8)	18.167(4)	106.37(3)	2	*C*2/*m*	2690/106	7
8	neyite	$Cu_2AgPb_{12.5}Bi_{13}S_{34}$	37.527(6)	4.0705(6)	43.701(7)	108.801(2)	4	*C*2/*m*	6319/250	8
9	vurroite	$Pb_{19.20}Sn_{1.42}Bi_{13.80}As_{9.58}S_{54}Cl_6$	45.502(9)	8.371(2)	27.273(6)	98.83(3)	4	*B*2/*b*	10265/416	9
10	synthetic	$Pb_2LaBi_6S_{14}$	21.2592(4)	4.0418(1)	28.1718(3)	-	4	*Pnma*	2421/92	10
11	synthetic	$TmCeS_3$	21.420(30)	3.98(1)	11.090(20)	102.90(20)	8	*P*2$_1$/*m*	922/40	11
12	synthetic	$Er_9La_{10}S_{26}$	29.710(10)	3.941(1)	21.830(10)	122.00(10)	2	*B*1 1 2/*m*	2168/90	12
13	synthetic	$Bi_2In_4S_9$	16.167(12)	3.917(2)	11.111(6)	94.044(3)	2	*P*1 2$_1$/*m* 1	702/30	13
14	synthetic	"$Pb_{8.67}Sb_{11.33}S_{23}$" (1)	50.570(10)	4.123(1)	22.263(4)	100.40(3)	4	*C*2	4566/≥172	14
15	synthetic	"$Cu_{0.51}Pb_{8.73}Sb_{8.15}I_{1.6}S_{20}$" (1)	49.801(4)	4.1132(8) (2)	21.989(1)	99.918(6)	-	monoclinic	4437/-	15

(1) This chemical composition is discussed in the text of the present paper. (2) A two-fold superstructure was detected. References: 1) this study, 2) Palvadeau *et al.* (2004), 3) Meerschaut *et al.* (2001), 4) Orlandi *et al.* (2005), 5) Orlandi *et al.* (2007), 6) Moëlo *et al.* (2000), 7) Doussier *et al.* (2007), 8) Makovicky *et al.* (2001), 9) Pinto *et al.* (2008), 10) Iordanidis & Kanatzidis (2001), 11) Rodier (1977), 12) Carré & Laruelle (1973), 13) Chapuis *et al.* (1972), 14) Light (1997), 15) Kryukova *et al.* (2005).

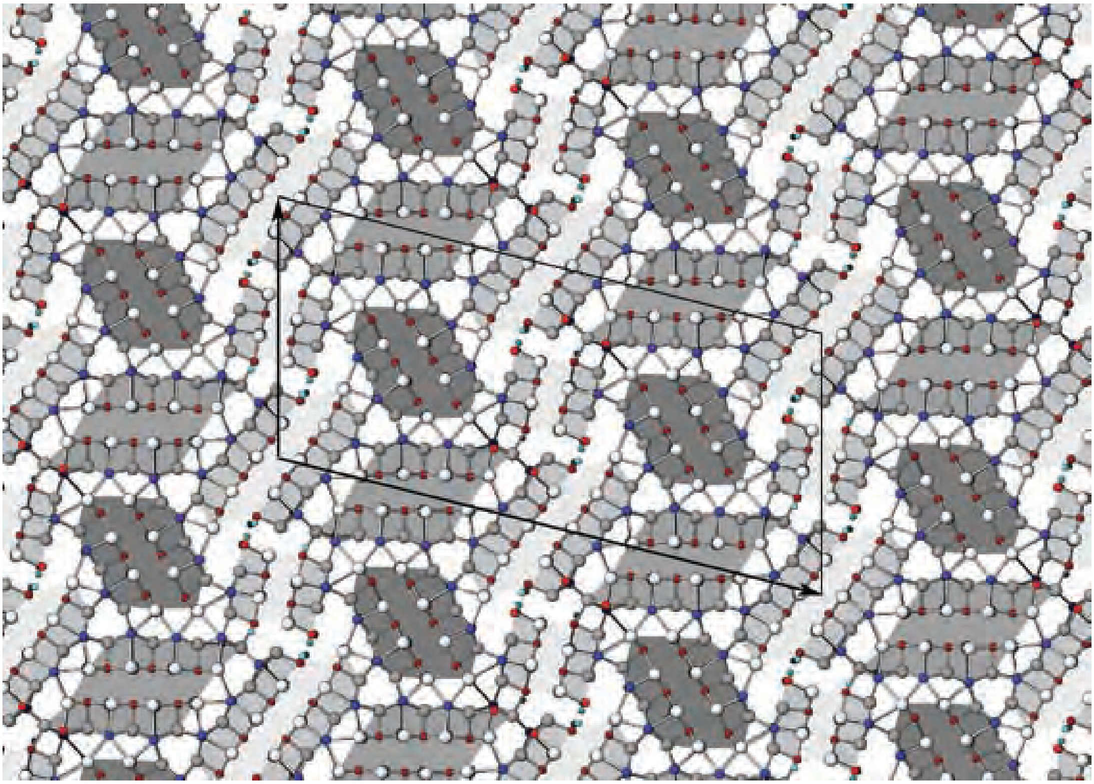

FIG. 3. The crystal structure of scainiite (Moëlo *et al.* 2000) with a high concentration of "kermesite-like configurations" along (001) planes, in continuation of "horizontal" interspaces. Oxygen is shown in light blue.

The *double layers* discernible in the wall structures based on SnS archetype take part in two adjacent rods. They are sinuous, as is also the layer in neyite, and start on one side of the wall, ending on its opposite side. Sinuosity is materialized *via* insertion of modified "kermesite-like fragments"(Moëlo *et al.* 2000) (in scainiite, Fig. 3), or by insertion of Hg (in marrucciite, Fig. 4), and by insertion of Pb [in pillaite (Fig. 5), which has three types of rods, although these layers (in "walls") can also be interpreted as Layer-type 11 of Makovicky (1993) with an extended "interconnecting" region between two adjacent rods, as well as in the present structure (Fig. 2)]. Finally, sinuosity can also be produced by the presence of slightly inflated lone-electron-pair micelles (in pellouxite, Fig. 6; for all references see Table 4). These sinuous double layers may have two types of termination: either both terminations end in Sb, which is coordinated to S *and* O in a "kermesite-type" arrangement defined by Moëlo *et al.* (2000) (see below), or they have one termination by a SbS_5 pyramid and another one of the "kermesite type". Each structure has only one type of double layers.

The *rods* constituting this wall-like structure are four atomic layers thick in all "typical" structures of the Pb–Sb category, the only exception being the central intervals of layers in pillaite. These rods follow $[010]_{SnS}$ in the case of pillaite, our sulfosalt, and the synthetic Mn sulfosalt (Fig. 7), whereas scainiite has rods parallel to $[001]_{SnS}$, and marrucciite has $[010]_{SnS}$ rods configurationally transitional to the PbS type and alternating with smaller PbS-type rods, which are centered on flattened HgS_6 octahedra (Orlandi *et al.* 2007, Laufek *et al.* 2007). In pellouxite, the $[001]_{SnS}$ and $[010]_{SnS}$ rods alternate along the layer. In the figures, these changes can be followed by noting the heights of anions on the opposing sides of lone-electron-pair micelles. The latter are indicated by shading that is lighter than that of the tightly bonded double-layers.

The lateral terminations of rods again are of two types: on the one hand, there are rods that end by means

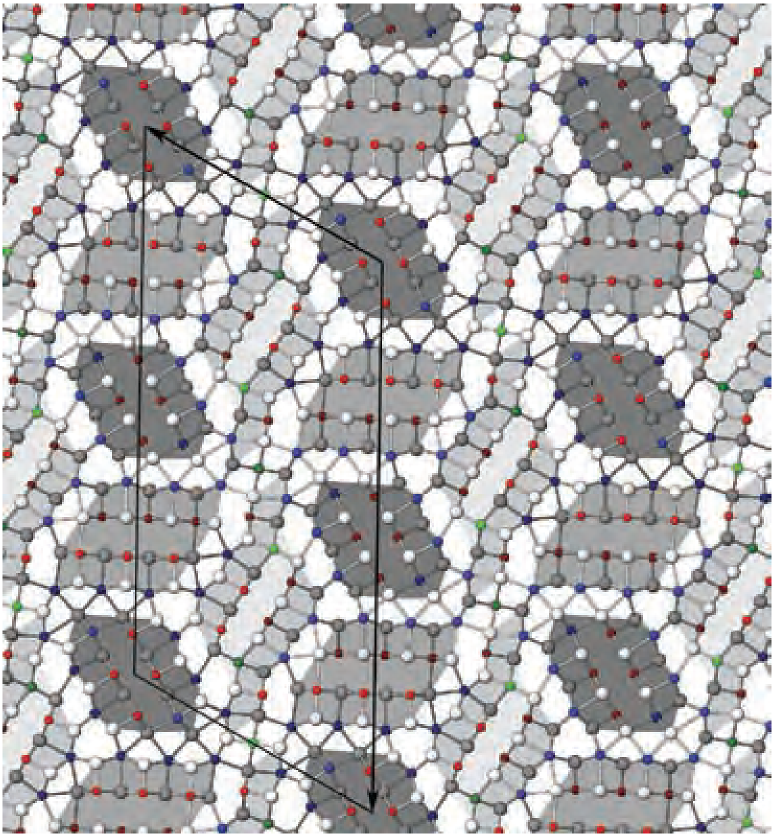

FIG. 4. The crystal structure of marrucciite (Orlandi *et al.* 2007) Note the two distinct flat-octahedron Hg sites in the vertical walls; it was left unshaded.

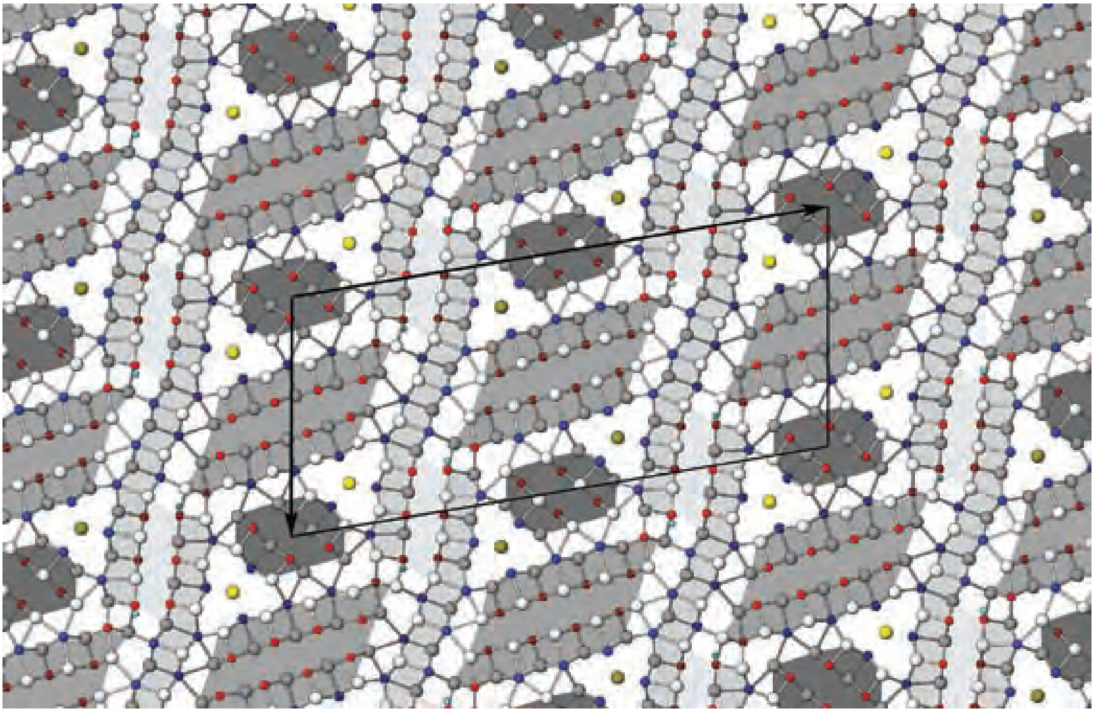

FIG. 5. The crystal structure of pillaite (Meerschaut *et al.* 2001). For conventions, see Figure 2. Rods of the walls (vertical) are terminated by "kermesite-like configurations", and box-fill rods are completed by chlorine atoms (yellow).

of anionic surfaces of $(101)_{SnS}$ type (in our structure, as well as in marrucciite and pellouxite), and on the other hand, those that are "truncated" by the "kermesite-like fragment", and lack the anionic-surface termination, which is common in rod-layer structures (Makovicky 1993). The latter type is represented by one type of rod in pellouxite, as well as by rods in pillaite, scainiite and the synthetic Mn sulfosalt.

The configuration of the *partitions* between the walls varies much less. In most cases, they are lozenge-shaped rods based on the SnS archetype, four atomic layers thick and with $[001]_{SnS}$ as the rod axis. The maximum width observed involves four pseudotetragonal subcells (pyramids) (pillaite); more common are three pyramids (*e.g.*, scainiite and the present compound), and a two-pyramid width is observed in the synthetic Mn sulfosalt. Their pseudohexagonal, anion-lined surfaces face the walls just described, the pseudotetragonal surfaces face the "fill" of the channels. The only other type observed are partitions in marrucciite; these are based on the PbS archetype and can be interpreted as truncated, with an additional Pb atom at the corner of the partition.

In neyite (Fig. 8) and in $La_{10}Er_9S_{27}$, dealt with in detail below, the partitions are pseudotetragonal layers, two atomic layers thick. In neyite, they contain a unique lateral offset in the form of a column of empty octahedra flanked by tetrahedrally coordinated Cu sites, fully analogous to the configurations observed in the sheared-layer structures of proudite-group minerals.

The *fill elements* (*contents of the boxes, "plugs"*) of the channels are rods of the SnS archetype in most structures. In neyite, they belong to the PbS archetype, and in rare-earth, lanthanum and indium–bismuth compounds, they are fragments of single-octahedron layers, *i.e.,* the PbS archetype as well. They are oriented with their anion surfaces toward the pseudotetragonal surfaces of the partitions, and with other anion surfaces toward the pseudotetragonal surfaces of the walls. As a rule, the extent of their pseudotetragonal surfaces is minimal; these occur at the spot where the fill elements face a termination of sinuous cation–anion (double-) layers from the walls. Two exceptions are known: a more extensive pseudotetragonal surface occurs in scainiite, in which the above "layer-termination region" is large, because it incorporates the local "kermesite-like fragment" with its surrounding configurations. An identical "fill element" is found in marrucciite, where the length of the layer-termination region of the wall structure is augmented by the coordination polyhedron of Hg.

The SnS-based "fill elements" are $[001]_{SnS}$ rods in most structures. In neyite (Makovicky *et al.* 2001), the synthetic Pb–La–Bi sulfosalt (Iordanidis & Kanatzidis

2001, Doussier *et al.* 2007) and the synthetic Mn sulfosalt (Doussier *et al.* 2007), as well as vurroite (Pinto *et al.* 2008) (the latter two examples contain single-octahedron rods), they are $[011]_{PbS}$. Because of different cross-sections, comparison of the size of fill elements in different structures can be best performed counting the number of cations and anions *per* cross-section in the projections illustrated. They start with MS_4 for single-octahedron columns and end with $M_{18}S_{26}$ for the present compound. For scainiite, the fill is M_9S_{14}, whereas in pillaite, the complete "fill" represents $M_6S_{10}Cl_2$, because chlorine completes the lozenge-shaped fill-rod. The same stoichiometry, M_6S_{12}, occurs in the PbS-like fragments, terminated by trigonal prisms, in $Pb_2La_xBi_{8-x}S_{14}$ (Iordanidis & Kanatzidis 2001, Doussier *et al.* 2007). In terms of an SnS-like arrangement, the rods of Sb sulfosalts contain between two fragments and four fragments of tightly bonded double layers, respectively seen in scainiite and in the new structure.

The different types of rods described here were already defined and illustrated by Moëlo *et al.* (2000) and Palvadeau *et al.* (2004) as rods A (defined as partitions in the present contribution), B (channel fill) and C_1–C_2 rods (Moëlo *et al.* 2000) or type-C ribbon layers (Palvadeau *et al.* 2004) (our walls). In the paper on marrucciite, Orlandi *et al.* (2007) altered the assignment of the A, B, C notation to the three rod types mentioned, and in the paper by Doussier *et al.* (2007), this notation was abandoned in favor of "palisade-like layers" discussed further below. A brief discussion of boxwork structures and illustration of the rods involved was also given by Ferraris *et al.* (2004) and Makovicky (2006).

Modular character of $Pb_{15-2x}Sb_{14+2x}S_{36}O_x$

The structure of $Pb_{15-2x}Sb_{14+2x}S_{36}O_x$ is a typical rod-based structure of a Pb–Sb boxwork type, broadly similar to those of pillaite or pellouxite, with the *largest*

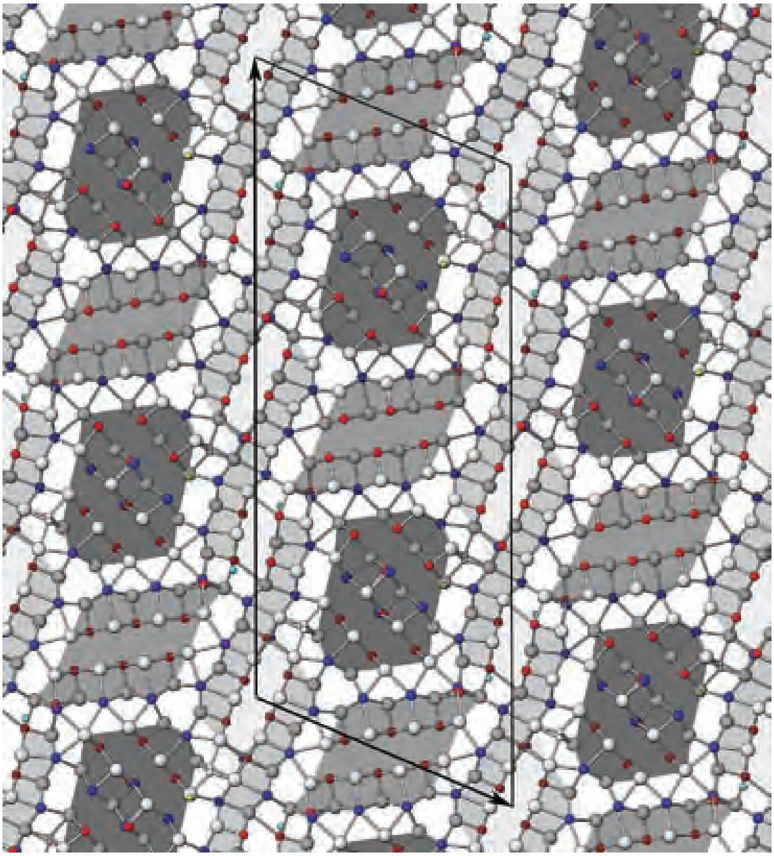

FIG. 6. The crystal structure of pellouxite (Palvadeau *et al.* 2004). Note the two distinct ways in which rods in the walls are terminated: by SbS_5 pyramids and by "kermesite-like" configurations, respectively. The latter allow deep insertion of rods forming horizontal partitions into the spaces created.

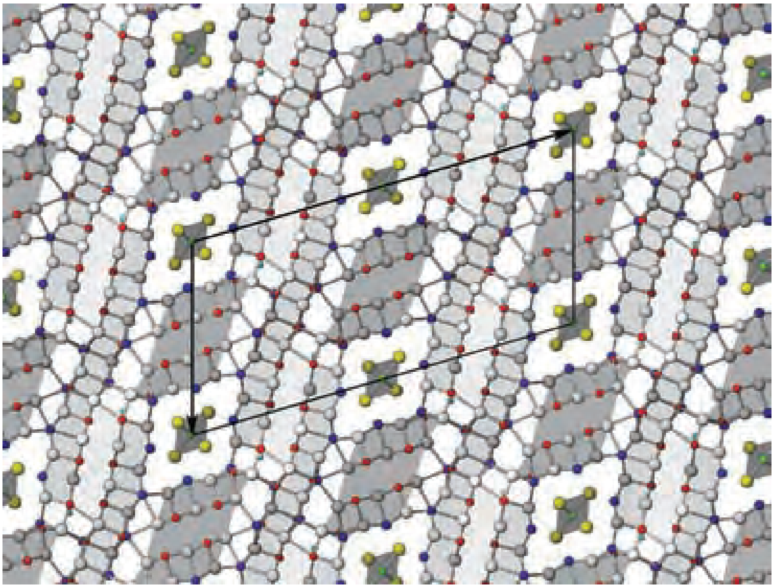

FIG. 7. The crystal structure of the synthetic Mn–Pb oxychlorosulfosalt (Doussier *et al.* 2007). Note the "kermesite-like configurations" in the walls and single-octahedron columns of (Mn,Pb)Cl_4 stoichiometry in the box interior.

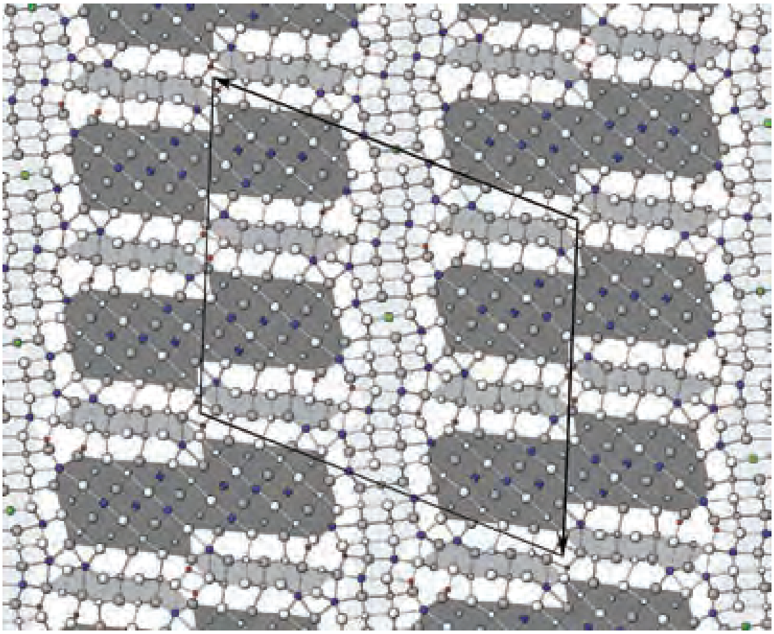

FIG. 8. The crystal structure of neyite (Makovicky *et al.* 2001). The Ag atom in the walls has a linear coordination, whereas Cu has tetrahedral and triangular coordination, respectively. Partitions (grey) and box-fill (dark grey) underwent crystallographic shear midway between walls.

channels or "*boxes*" and most voluminous channel fill known to this day (Table 4). Typically, rods of the box walls and partitions are primarily rods with extensive pseudotetragonal surfaces. Sheared pseudohexagonal surfaces $3^3.4^2$ form only portions of rod terminations. Correspondingly, the box contents consist of an enclosed rod with all surfaces of a sheared pseudohexagonal type, with only single-corner pyramids as intervals of pseudotetragonal type (Fig. 2).

The combined (100) *walls* in $Pb_{15-2x}Sb_{14+2x}S_{36}O_x$ consist of two alternating types of rods arranged *en échelon* in a way similar to the rod-layers in boulangerite: (1) smaller rods, with four combined layers of cations–anions that are three coordination pyramids wide [these are pseudotetragonal pyramids that have also been described as Q subcells by Makovicky (1993)]. They are interconnected with (2) larger rods *via* tightly bonded double-layers. The latter rods are 3½ pyramids wide, 4 atomic layers thick, and they end in "kermesite-like portions", instead of the classical $3^3.4^2\,(101)_{SnS}$ endings [a mathematical notation for surfaces in which three triangular and two quadratic configurations of sulfur atoms meet in every S atom, defined as sheared pseudohexagonal anionic surfaces by Makovicky (1993)], seen in the classical rod-based sulfosalts (Makovicky 1993). In this "kermesite-like" configuration, the horizontal, outwardly oriented short Sb–S bond and that to the vertex of the pyramid are accompanied by a short bond to oxygen above or below the Sb atom.

The partition (quoted as rod category 3 below) is a rod that is three pseudotetragonal coordination pyramids wide; it has a regular rod aspect and a lozenge-like cross-section. *The encapsulated "fill" rods* (category 4) are eight atomic layers thick, and in their principal portions, they are three pyramids wide, with terminal double-layers reduced to a width of two, and finally only one coordination pyramid (Fig. 2). The anionic surfaces are of the $3^3.4^2$ configuration; the rod is truncated in two opposing corners by pseudotetragonal intervals only one Pb pyramid wide.

Rods of the categories (1) and (2) are infinite along $[010]_{SnS}$, whereas the category (3), *i.e.*, the transversal rod (*i.e.*, the partition) and (4) the boxwork infill, are infinite along $[001]_{SnS}$. In the projection along [010] of the present structure, the cases (1) and (2) exhibit "lying-down" monocapped trigonal coordination prisms, whereas the configurations (3) and (4) are composed of "standing" monocapped trigonal coordination prisms (Fig. 2). The Sb–S–O configuration of rods (2) forms an embayment into which a corner of the transversal rod (3) is inserted.

The degenerate cyclic character (Makovicky 1985, Moëlo *et al.* 2000) of the structure of $Pb_{15-2x}Sb_{14+2x}S_{36}O_x$ is produced by the arrangement of three distinct rods around a local three-fold axis in each of the acute corners of a "boxwork" channel. On a local scale, they form groups of three edge-sharing bicapped trigonal coordination prisms of Pb. The rods involved are of the category (1) and (3) defined above, both of 3Q type, but with different external connections, as well as the corner portions of the large rod (4). As mentioned above, the rods (1) and (3) display an orientation of the SnS archetype at 90° to that in rod (4). All this limits the size of the region that obeys the local three-fold axis.

Surfaces of the first three types of rods in $Pb_{15-2x}Sb_{14+2x}S_{36}O_x$ are occupied by Pb in standing and lying-down trigonal coordination prisms, which are mono-, bi-, and tricapped, according to the local match requirement on rod interfaces. The longest match is ~4 Q : 2½ H in terms of primitive pseudotetragonal (Q) and centered orthohexagonal (H) subcells (mesh), followed by ~2½ Q : 1½ H and ~1½ Q : 1 H. Rods of category (1) and (2) together compose a (100) *rod-layer* that approximates the Type-1 rod-layer of Makovicky (1993), although modified by the insertion of a "kermesite-like configuration" at selected edges. The configurations resulting from this arrangement allow insertion of an unmodified transversal 3Q rod (a partition) and a formation of a "box", in which the cation–anion contacts between the walls and "fill" satisfy the coordination requirements of lead.

STRUCTURAL AFFINITIES OF $Pb_{15-2x}Sb_{14+2x}S_{36}O_x$

If we consider the number of strongly bonded double-layers present in the box-fill of the Pb–Sb sulfosalts, the new oxysulfosalt presents four, rouxelite three, and scainiite, marrucciite and pellouxite only two double-layers each, separated in all cases by lone-electron interspaces. The situation in pellouxite is modified by the "termination" of the lozenge-like infill by columns of chlorine atoms. These are situated in those portions of the structure already occupied by the framework of the walls and partitions in scainiite and marrucciite. In this context, the columns of octahedra in vurroite and in the synthetic Mn sulfosalt can be interpreted as one double-layer plus one interspace.

This concept leads to the question of possible homologous series in this group of compounds. All representatives of the Pb–Sb sulfosalts of the "core" oxysulfosalt group, related to zinkenite, have variously large local environments in common, as illustrated in the original descriptions by the Nantes–Pisa research group. However, the misfit between the dimensions of the arrays of pseudotetragonal subcells in the walls and the dimensions of the $n \times (101)_{SnS}$ subperiodicity of pseudohexagonal surfaces means that practically all attempts to produce a homologous expansion or contraction are frustrated, demanding excessive concentrations of kermesite-like elements in order to compensate for the lack of fit.

The new sulfosalt, $Pb_{15-2x}Sb_{14+2x}S_{36}O_x$, however, represents a case close to homology. In the structure of pellouxite (Palvadeau *et al.* 2004), a large complex rod (Fig. 9) can be defined, which also describes large portions of the structure of $Pb_{15-2x}Sb_{14+2x}S_{36}O_x$. The latter structure contains additional elements that form a zig-zag layer cutting diagonally through the walls and the box-fill and displacing the complex rods as well (Fig. 9). In addition, however, when we proceed along the [100] and [001] directions of pellouxite, the adjacent complex rods are invariably displaced by ½Q (~2 Å) parallel to [010] in the new compound. Therefore, these two structures are not two homologues in an exact sense but plesiotypes (Makovicky 1997).

From the Rod-Based to Boxwork Structures: the Importance of the "Kermesite-like" Configuration

Makovicky (1993) demonstrated that the non-commensurate match of pseudotetragonal and pseudohexagonal surfaces of adjacent structural elements (rods) in the rod-layer sulfosalt structures leads to a definite and limited selection of rod shapes and sizes that can be combined in one structure; similar limitations exist for the chessboard type of rod-based structures. By now, this selection has been about completely covered by the known sulfosalts of those cations that are available in nature. The key to the existence of additional *new* sulfosalts, especially of antimony, is the presence of a "kermesite-like configuration" (Fig. 10), first defined by Moëlo *et al.* (2000), and mentioned briefly several times in the preceding text.

What is this "kermesite-like configuration"? The peripheral Sb atom of an aggregate of Sb–S coordination pyramids (*i.e.*, of a rod) typically has a square-pyramidal coordination SbS_5, with an apically oriented pair of short Sb–S bonds in the base of the pyramid; these are at 45° to the rod extension. In the "kermesite-like" configuration (Moëlo *et al.* 2000), however, it has only one such outwardly oriented bond, at about 90° to the rod extension. In the "apically" situated "kermesite-like"configurations, it is a bond to S, but in the paired fragments inside the walls in scainiite, it is a bond to the oxygen of the opposing kermesite-like configuration (Fig. 10). The Sb–S bond to the (original) pyramid vertex remains preserved, and the triplet of mutually perpendicular short Sb–anion bonds, typical for Sb^{3+}, is completed by a bond to an oxygen atom above or below the Sb atom, along the rod extension. The latter choice can be statistical, at least on the level of entire structure. Moëlo *et al.* (2000) gave this configuration its name

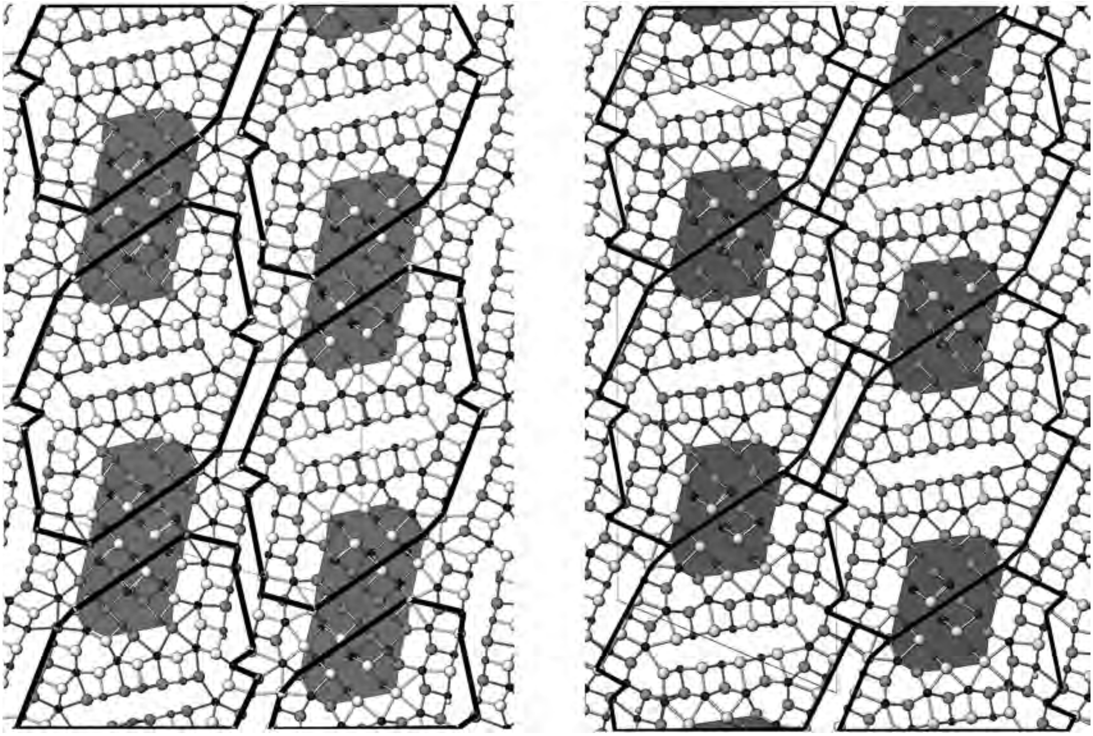

FIG. 9. Rod configurations common to $Pb_{15-2x}Sb_{14+2x}S_{36}O_x$ (left) and pellouxite (right). Note the mutual shifts in the heights of rods by 2 Å, when proceeding along either crystallographic direction. They are different in the two phases and are expressed by coloring of atoms (light and dark). Note also the additional structure portions present in $Pb_{15-2x}Sb_{14+2x}S_{36}O_x$.

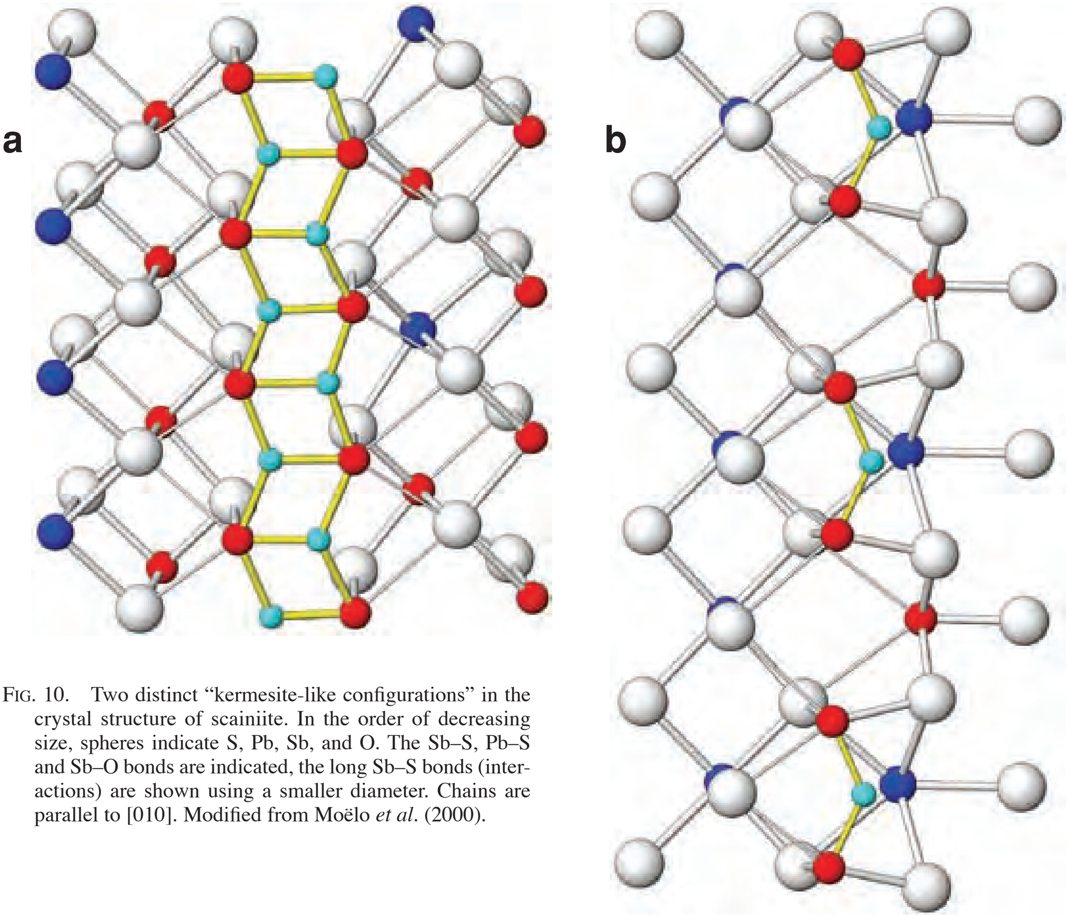

FIG. 10. Two distinct "kermesite-like configurations" in the crystal structure of scainiite. In the order of decreasing size, spheres indicate S, Pb, Sb, and O. The Sb–S, Pb–S and Sb–O bonds are indicated, the long Sb–S bonds (interactions) are shown using a smaller diameter. Chains are parallel to [010]. Modified from Moëlo *et al.* (2000).

because of its *general* similarity to apical interconnections of sulfide–oxide ribbons in kermesite, Sb_2S_2O (Kupčík 1967, Bonazzi *et al.* 1987, Ďurovič & Hybler 2006). Details of atom coordinations (bond distances) in the "kermesite-like" configurations of Pb–Sb oxysulfosalts are to be found in Moëlo *et al.* (2000), Orlandi *et al.* (2001, 2004) and Doussier *et al.* (2007).

Both the apically or internally situated "kermesite configurations" *shorten the pseudotetragonal subperiodicity* of cation–anion configurations (and their surfaces) by about a half-width of the coordination pyramid of Sb, in the direction perpendicular to the rod orientation. Thus, the structural element that follows, and is attached into the embayment of the structure wall, can be positioned "earlier", and yield structural configurations not considered possible with the above-mentioned "classical matches" in rod-based sulfosalts. In addition, as already mentioned by Moëlo *et al.* (2000), the paired "kermesite-like" elements in the centers of double layers in scainiite shift the two portions of the double layer by ~2 Å against one another. For the Pb–Sb sulfosalts, along the wall direction, the position of the next *partition* thus fits with the dimensions and position of the *fill element* and can follow after it. It would be situated too far for any contact with the fill element without the intervention of the "kermesite fragment". Furthermore, the "horizontally situated" apical S atom of the "kermesite configuration" becomes a regular corner-component of the partition (Figs. 2, 3), and determines its shift along the rod axis to such a level that the coordinations of Pb atoms on the partition surfaces fit with the heights of S atoms on the pseudohexagonal surfaces of the fill element. All this would not exist without the small islands of "kermesite configuration" in the structure.

Is oxygen invariably present? Light (1997) described a structure of "$Pb_{8.67}Sb_{11.33}S_{23}$", with a nonstoichiometric formula derived from structure determination, with unit-cell dimensions (Table 4) marginally larger than those of pillaite (Meerschaut *et al.* 2001) and a crystal structure virtually identical with that of pillaite. Light placed an Sb atom (with 5% Pb) into the Cl site of pillaite; all metal and metalloid sites were refined as mixed sites. These crystals are a product of vapor transport with iodine and H_2O vapor as a transport medium. Thus, we interpret this "trigonal prismatic Sb position" as the *iodine position*, the "5% Pb content" being in full agreement with the difference between the atomic numbers of Sb and I. The I–cation distances are 3.514 Å, 3.546 Å, and 3.610 Å, to be compared with the Cl-cation distances in pillaite itself, 3.250 Å, 3.329 Å, and 3.399 Å. The marginal Sb atom in the rods of the continuous walls in Light's structure has a coordination identical to that in the "kermesite configurations" of pillaite, except for the *unidentified oxygen*.

Our interpretation of the phase synthesized by Light (1997) has been corroborated by the syntheses of Kryukova *et al.* (2005), who prepared a phase with unit-cell parameters nearly identical with those of pillaite (Table 4), a composition estimated by a combination of WDS and EDS as $Cu_{0.51}Pb_{8.73}Sb_{8.15}I_{1.6}S_{20}$ (no data on the analysis given; the phase was obtained by vapor transport from a natural, mixed sulfosalt material), and a pillaite-like structure that was verified by HRTEM and comparison of calculated and observed powder-diffraction patterns. Therefore, both sets of investigations describe apparently the same phase, a synthetic "iodo-pillaite", and left some problems unsolved, especially *the presence of oxygen* in the "kermesite-like fragments", which seems inevitable from the coordination found by Light (1997).

PALISADE-LIKE LAYERS ("COUCHES GAUFRÉES")

As already mentioned, Moëlo *et al.* (2000) and the authors of later publications of the Nantes–Pisa group used another type of layer definition than used here. They drew a "complex rod layer", in which rods are the above-mentioned boxes with their fill, and include the adjacent halves of walls. Boundaries of these layers (called by them "*couches gaufrées"*) pass *wherever possible* through lone-electron-pair micelles and through interfaces between archetype rods as defined by us. Doussier *et al.* (2007) calls such a layer "*a palisade-like layer* with a waffle structure". Layers so defined follow the presumed easy cleavage of these Pb–Sb sulfosalts. This principle of structure slicing, which preserves tightly bonded elements, reflects yet another aspect of the Pb–Sb subfamily of boxwork sulfosalts. It uses a quite different definition of a "rod", and the channel infill becomes a "lozenge heart". The concept of Doussier *et al.* does not lead to the recognition of the SnS-based character of the structure. The extension of the waffle layer concept by Doussier *et al.* (2007) to channel structures with tightly bonded walls, where a waffle layer is not individualized [such as $Pb_4La_{2x}Bi_{16-2x}S_{28}$ (Iordanidis & Kanatzidis 2001), treated further below] and has to be cut out of the strong, three-dimensionally continuous porous framework, gives a definition of waffle structures that differs from the one given at the beginning of their paper.

The paper by Doussier *et al.* (2007) contains an attempt to classify boxwork structures according to the complex palisade-like layers in them, distancing them in this way from the large body of rod-based structures of layer, chessboard, and even cyclic types. One of the aims of the present paper is to re-establish this connection, preserving the unity of the family of rod-based structures on a higher level of complexity.

STRUCTURE TYPES OTHER THAN PB–SB OXYSULFOSALTS RELATED TO ZINKENITE

Vurroite, $Pb_{10}Sn(Bi,As)_{11}S_{27}Cl_3$ (Pinto *et al.* 2008) is a boxwork structure with single octahedron columns $(Sn,Bi)_4$ in boxes of lozenge-like cross-section (Fig. 11). The walls consist of rods, two and three (As,Bi) pyramids wide, arranged into tiers by intercalated planes of trigonally coordinated Pb and mixed-cation positions. These levels also act as mirror planes of the motif, so that no clear distinction into walls and partitions can be made.

The structure of *rouxelite* (Orlandi *et al.* 2005) (Fig. 12) deviates most from the above "core" group. The principal walls are composed of three quasicontinuous cation–anion planes, to which short, alternately positioned intervals of the fourth plane are added in a way similar to the PbS-based rods in kobellite. The lone-electron-pair micelle enclosed in the three-plane layer fluctuates in accordance with these additions. Between these layers, stacks of two alternating types of rods are packed: (1) truncated lozenges, four pyramids wide, and based on the PbS archetype, and (2) S-shaped rods, which contain eight atomic planes and remind one of the rod configuration seen in kobellite as well (Orlandi *et al.* 2005). In rouxelite, however, they are based on the SnS archetype.

The quasicontinuous layer of rouxelite incorporates foreshortened, skewed coordination octahedra of Hg, which inflates its subperiods locally, in the layer center, rotating the associated coordination polyhedra in the process. These then create "prongs" of an appropriately reduced size on layer surfaces, suitable for inception of Cu tetrahedra. Layer portions with these elements alternate with the portions containing seven-coordinated antimony, which mimic exactly the "kermesite-like portions" described above. They shorten the layer and displace periodically its intervals by 2 Å along [010], bringing them into the right level of attachment for the adjacent rods.

Neyite, $Ag_2Cu_6Pb_{25}Bi_{26}S_{68}$ (Makovicky *et al.* 2001), is a type structure of the boxwork concept (Fig. 8). The clearly outlined box-fill is of the PbS type, with the composition $M_{26}S_{36}$ and with pseudohexagonal surfaces, disturbed only by two short Q intervals at the acute corners. The boxfill faces the pseudotetragonal

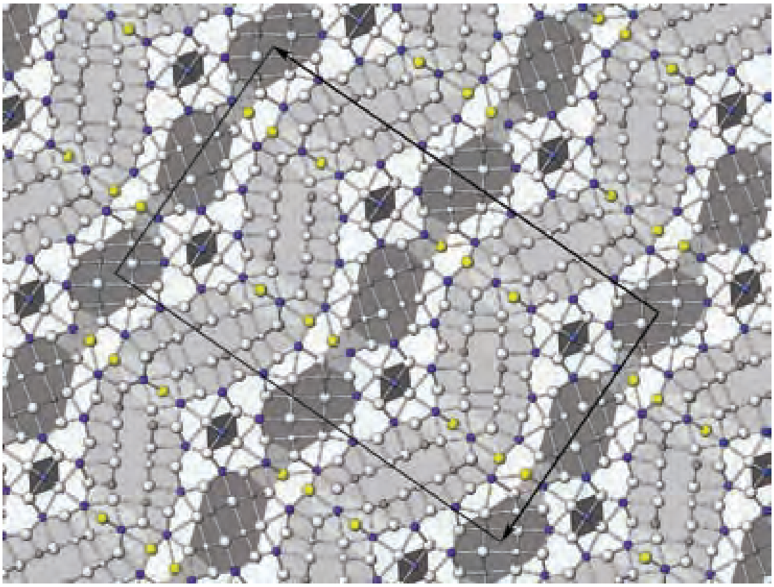

FIG. 11. The crystal structure of vurroite (Pinto *et al*. 2008). Two kinds of walls, respectively composed of rods, two and three pyramids wide (indicated by two kinds of shading), enclose boxes with a single-octahedron (Sn, Bi) fill.

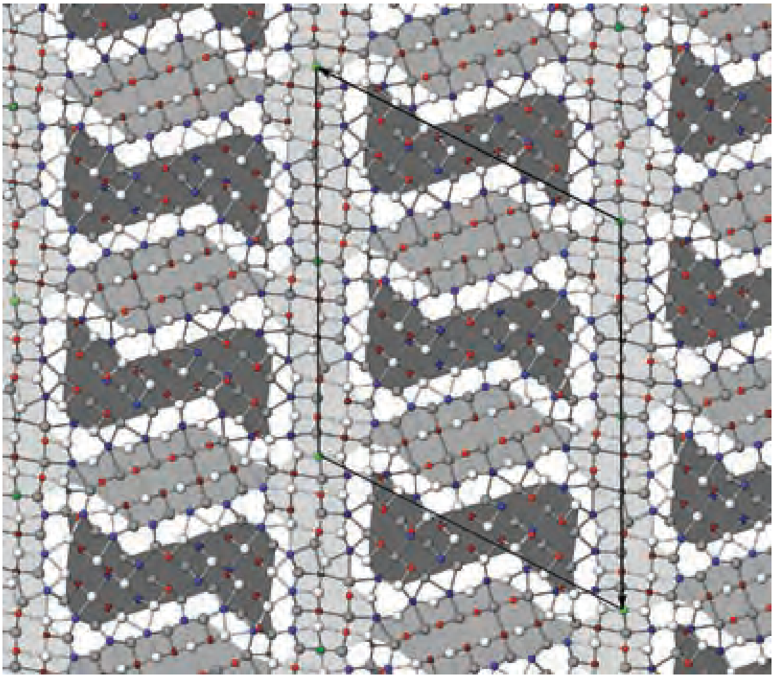

FIG. 12. The crystal structure of rouxelite (Orlandi *et al*. 2005). Note the flattened octahedron of Hg and the tetrahedrally coordinated Cu atoms. There are three kinds of modules, which lead to a local but not a global kinship to the kobellite structure-type. Details are in the text.

surfaces of the sinuous walls, three atomic planes thick, as well as those of the tightly bonded double-layers serving as partitions. In analogy to rouxelite, the straight portions of the sinuous walls are locally extended by insertion of broad, foreshortened Ag octahedra, and the four surrounding polyhedra are rotated and thus fitted to the periodicity of the adjacent pseudohexagonal surface (Fig. 8).

One of the smallest boxwork frameworks among sulfosalts is the structure of $Bi_2In_4S_9$ (Chapuis *et al.* 1972). Ribbons with a composition $Bi_2In_2S_6$ form porous walls; other such ribbons, stabilized in place by In–S bonds, form partitions, and fragments of octahedrally coordinated In layers are the box fill (Fig. 13). The marginal atoms of five-coordinated indium in the latter fragments can be assigned either to the framework or to the fill.

Another sulfosalt, $Pb_4La_{2x}Bi_{16-2x}S_{28}$ (Iordanidis & Kanatzidis 2001), is a typical boxwork-type structure with tightly bonded double-walls and lozenge-shaped channels, which contain four octahedra and two trigonal coordination prisms of bismuth per unit volume, fitting perfectly into the box area (Fig. 14). This structure was also treated by Doussier *et al.* (2007), together with the La–Bi sulfosalt mentioned below. At the crossing of the walls, a group of two monocapped lying-down and two bicapped standing prisms occur, as in $PbBi_2S_4$ and Gd_2S_3. The latter group, consisting ideally of two Bi and two Pb (REE) polyhedra, or just of four large REE-bearing polyhedra, will be seen in the REE sulfide structures as well. The structure of $La_8Bi_4S_{18}$ (Ecrepont *et al.* 1988) is similar in principle to that of $Pb_4La_{2x}Bi_{16-2x}S_{28}$. It displays smaller boxes, which contain only double-octahedron columns of stoichiometry Bi_2S_6.

Two rare-earth-element structures of boxwork type, in which large and small REE are combined in the same structure, are $La_{10}Er_9S_{27}$ (Carré & Laruelle 1973) and $CeTmS_3$ (Rodier 1973), illustrated in Figures 15 and 16, respectively. Walls are complex, with a distinct role for the above-mentioned combinations of prisms, partitions are pseudotetragonal double-layers, and the box fill involves fragments of layers of octahedra, three and two octahedra wide, respectively.

CONCLUSIONS

Considering the volume and the contents of the boxes created by the framework of boxwork structures, $Pb_{15-2x}Sb_{14+2x}S_{36}O_x$ and neyite are the largest structures of this remarkable family of *boxwork structures*, all of which display a segregation of a simple, archetypal rod inside a complex structural arrangement. For the majority of Pb–Sb sulfosalts that belong to this category, including $Pb_{15-2x}Sb_{14+2x}S_{36}O_x$, the structural arrangement becomes possible only by insertion of oxygen, which generates so-called "kermesite-like configurations" that serve as *structure modifiers,* with a profound influence on the fit of structure modules and on the resulting periodicity of the structure. In other structures of this family, the role of the *structure modifier* is played by Hg or Ag. The principal walls of many of these frameworks commonly are complex structures by them-

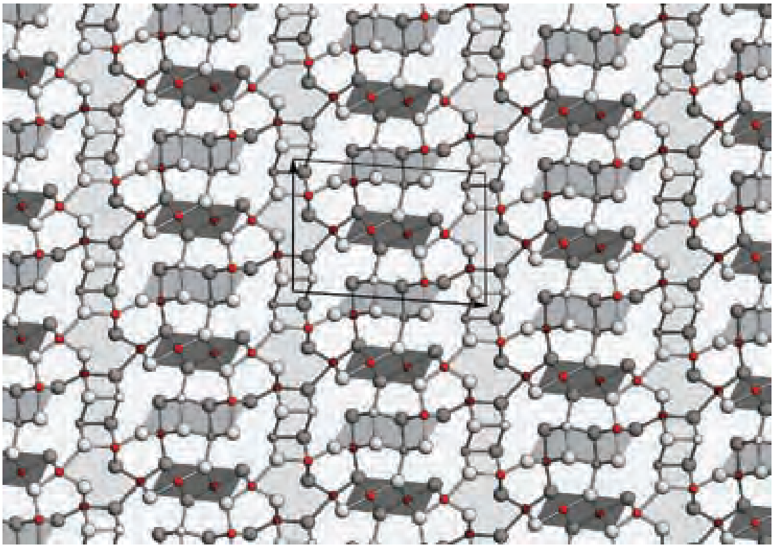

FIG. 13. The crystal structure of $Bi_2In_4S_9$ (Chapuis *et al.* 1972) with six- and five-coordinated indium, and square-pyramidal Bi. Three kinds of elements are present: "porous" walls (vertical), partitions and double-octahedron chains as a fill.

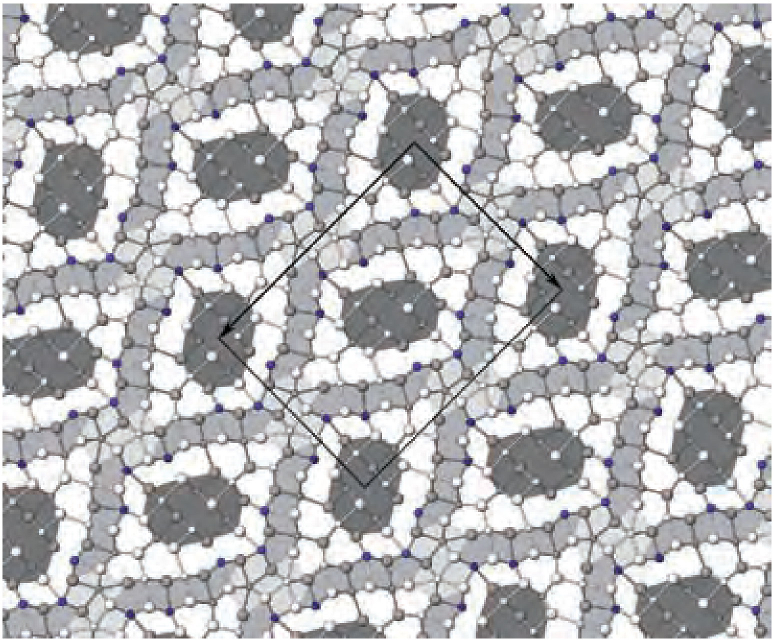

FIG. 14. The crystal structure of the synthetic Pb–La–Bi sulfosalt (Iordanidis & Kanatzidis 2001). The boxwork consists of two-sheet-thick pseudotetragonal walls with no obvious division into walls and partitions, and a seven-coordinated cation in wall intersections.

selves, but the partitions interconnecting them are rather simple, four or only two atomic layers thick, and the box fill (apparently) in all cases are simple rods based on the SnS or PbS archetype. For the Pb–Sb sulfosalts, rods built both along [001] and along [010] directions of the SnS archetype can be present as different elements of the same structure, a phenomenon nearly absent in rod-layer structures described by Makovicky (1993). Up to four distinct types of rods, in the sense of Makovicky (1993, 1997), can combine in one boxwork structure. In spite of a number of common structure features, the Pb–Sb oxysulfosalts related to zinkenite do not form true homologous series or pairs.

ACKNOWLEDGEMENTS

This research was supported by grant no. 21–03–0519 of the State Research Council for Natural Sciences (Denmark) and by Christian Doppler Forschungsgesellschaft (Austria). Thorough reviews by Dr. Yves Moëlo and Dr. Allan Pring, as well as the editorial care of Prof. R.F. Martin, are gratefully acknowledged.

REFERENCES

BERLEPSCH, P., MAKOVICKY, E. & BALIĆ-ŽUNIĆ, T. (2001): Crystal chemistry of sartorite homologues and related sulfosalts. *Neues Jahrb. Mineral., Abh.* **176**, 45-66.

BONAZZI, P., MENCHETTI, S. & SABELLI, C. (1987): Structure refinement of kermesite: symmetry, twinning and comparison with stibnite. *Neues Jahrb. Mineral., Monatsh.*, 557-567.

CARRÉ, D. & LARUELLE, P. (1973): Structure cristalline du sulfure d'erbium et de lanthane, $Er_9La_{10}S_{27}$. *Acta Crystallogr.* **B29**, 70-73.

CHAPUIS, G., GNEHM, C. & KRÄMER, V. (1972): Crystal structure and crystal chemistry of bismuth indium sulfide, $Bi_2In_4S_9$. *Acta Crystallogr.* **B28**, 3128-3130.

DOUSSIER, C., MOËLO, Y., LÉONE, P. & MEERSCHAUT, A. (2007): $(Mn_{1-x}Pb_x)Pb_{10+y}Sb_{12-y}S_{26-y}Cl_{4+y}O$, a new oxychloro-sulfide with ~2 nm-spaced (Mn,Pb)Cl_4 single chains within a waffle-type structure. *J. Solid State Chem.* **180**, 2323-2334.

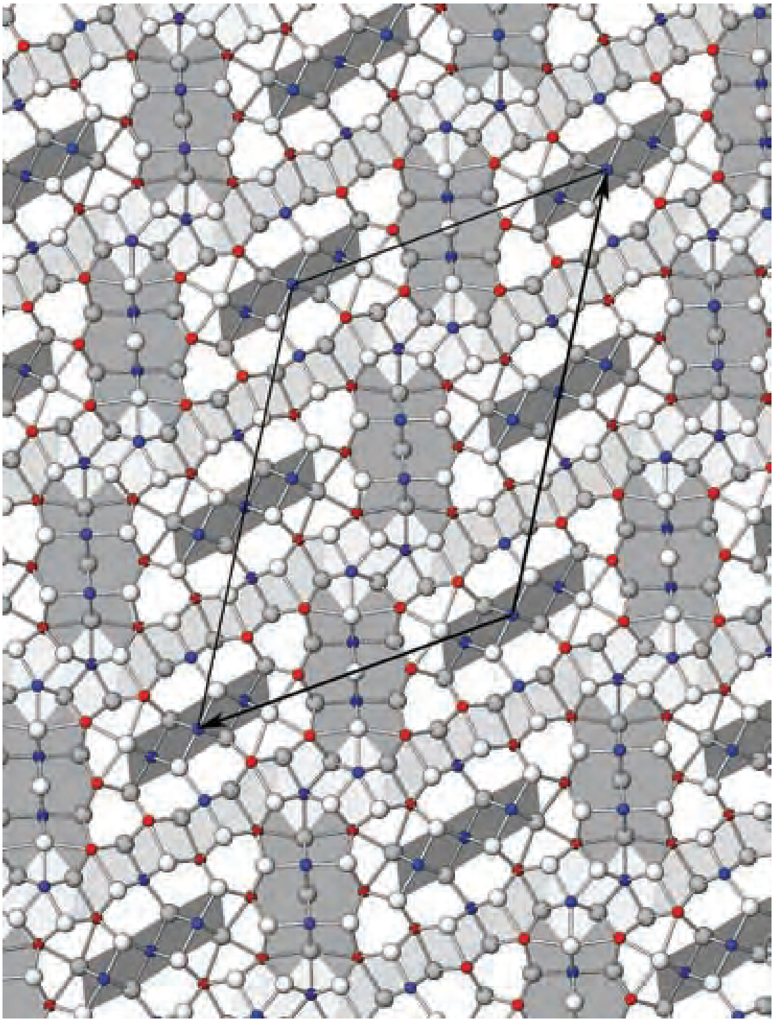

FIG. 15. The crystal structure of $Er_9La_{10}S_{27}$ (Carré & Laruelle 1973). Walls underwent a homologous expansion in comparison to those in Figure 14, partitions have greater length, and the filling elements are three-strand ribbons of octahedra. A conspicuous configurational affinity exists to the sulfosalt structure in Figure 14.

ĎUROVIČ, S. & HYBLER, J. (2006): OD structures in crystallography – basic concepts and suggestions for practice. *Z. Kristallogr.* **221**, 63-76.

ECREPONT, C., GUITTARD, M. & FLAHAUT, J. (1988): Système $La_{4/2}S_3$–Bi_2S_3: phases intermédiaires; diagramme de phase. *Mater. Res. Bull.* **23**, 37-42.

FERRARIS, G., MAKOVICKY, E. & MERLINO, S. (2004): *Crystallography of Modular Materials*. Oxford University Press, Oxford, U.K.

HOFMANN, W. (1933): Die Struktur der Minerale der Antimonitgruppe. *Z. Kristallogr.* **86**, 225-245.

IORDANIDIS, L. & KANATZIDIS, M.G. (2001): Novel quaternary lanthanum bismuth sulfides $Pb_2 La_x Bi_{8-x} S_{14}$, $Sr_2La_x Bi_{8-x} S_{14}$, and $Cs_2 La_x Bi_{10-x} S_{16}$ with complex structures. *Inorg. Chem.* **40**, 1878-1887.

KRYUKOVA, G.N., HEUER, M., WAGNER, G., DOERING, T. & BENTE, K. (2005): Synthetic $Cu_{0.507(5)}Pb_{8.73(9)}Sb_{8.15(8)} I_{1.6}S_{20.0(2)}$ nanowires. *J. Solid State Chem.* **178**, 376-381.

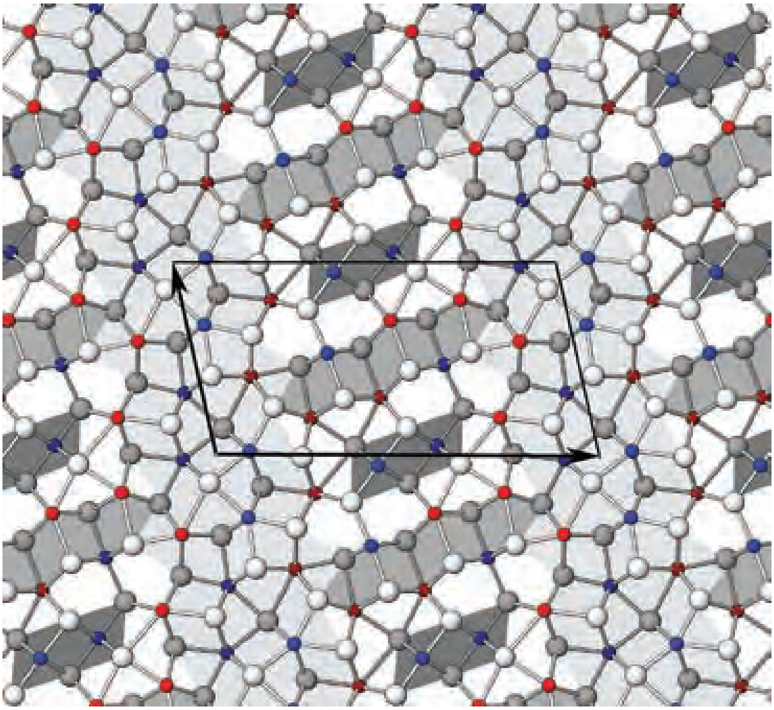

FIG. 16. The crystal structure of $CeTmS_3$ (Rodier 1973). It has complex walls (see text), simple partitions, and octahedron elements of the boxfill similar to, but narrower than, those in Figure 14. Cerium prefers a bicapped trigonal prismatic coordination, whereas Tm prefers coordination by six and seven ligands.

KUPČÍK, V. (1967): Die Kristallstruktur des Kermesits, Sb_2S_2O. *Naturwiss.* **54**, 114.

LAUFEK, F., SEJKORA, J., FEJFAROVÁ, K., DUŠEK, M. & OZDÍN, D. (2007): The mineral marrucciite: monoclinic $Hg_3Pb_{16}Sb_{18}S_{46}$. *Acta Crystallogr.* **E63**, i190 [doi:10.1107/S1600536806040980].

LIGHT, M.E. (1997): *Structural Studies of Mineral Silicates and Synthetic Sulfosalts Characterised by Mixed Occupancies*. Ph.D. thesis, Univ. of Wales, Cardiff, U.K.

MAKOVICKY, E. (1985): Cyclically twinned sulfosalt structures and their approximate analogues. *Z. Kristallogr.* **173**, 1-23.

MAKOVICKY, E. (1992): Crystal structures of complex lanthanide sulfides with built-in non-commensurability. *Aust. J. Chem.* **45**, 1451-1472.

MAKOVICKY, E. (1993): Rod-based sulphosalt structures. *Eur. J. Mineral.* **5**, 545-591.

MAKOVICKY, E. (1997): Modular crystal chemistry of sulphosalts and other complex sulphides. *In* Modular Aspects of Minerals (S. Merlino, ed.). *Eur. Mineral. Union, Notes in Mineralogy* **1**, 237-271.

MAKOVICKY, E. (2005): Micro- and mesoporous sulfide and selenide structures. *In* Micro- and Mesoporous Mineral Phases (G. Ferraris & S. Merlino, eds.). *Rev. Mineral. Geochem.* **57**, 403-433.

MAKOVICKY, E. (2006): Crystal structures of sulfides and other chalcogenides. *In* Sulfide Mineralogy and Geochemistry (D.J. Vaughan, ed.). *Rev. Mineral. Geochem.* **61**, 7-125.

MAKOVICKY, E., BALIĆ-ŽUNIĆ, T. & TOPA, D. (2001): The crystal structure of neyite, $Ag_2Cu_6 Pb_{25} Bi_{26} S_{68}$. *Can. Mineral.* **39**, 1365-1376.

MAKOVICKY, E. & MUMME, W.G. (1986): The crystal structure of izoklakeite, $Pb_{51.3}Sb_{20.4} Bi_{19.5} Ag_{1.2}Cu_{2.9} Fe_{0.7} S_{114}$. The kobellite homologous series and its derivatives. *Neues Jahrb. Mineral., Abh.* **153**, 121-145.

MAKOVICKY, E., TOPA, D. & MUMME, W.G. (2006): The crystal structure of dadsonite. *Can. Mineral.* **44**, 1499-1512.

MEERSCHAUT, A., PALVADEAU, P., MOËLO, Y. & ORLANDI, P. (2001): Lead–antimony sulfosalts from Tuscany (Italy). IV.

Crystal structure of pillaite, $Pb_9Sb_{10}S_{23}ClO_{0.5}$, an expanded monoclinic derivative of hexagonal $Bi(Bi_2S_3)_9I_3$, from the zinkenite group. *Eur. J. Mineral.* **13**, 779-790.

Miehe, G. (1971): Crystal structure of kobellite. *Nature Phys. Sci.* **231**, 133-134.

Moëlo, Y., Makovicky, E., Mozgova, N.N., Jambor, J.L., Cook, N., Pring, A., Paar, W., Nickel, E.H., Graeser, S., Karup-Møller, S., Balić-Žunić, T., Mumme, W.G., Vurro, F., Topa, D., Bindi, L., Bente, K. & Shimizu, M. (2008): Sulfosalt systematics: a review. Report of the sulfosalt sub-committee of the IMA Commission on Ore Mineralogy. *Eur. J. Mineral.* **20**, 7-62.

Moëlo, Y., Meerschaut, A.,Orlandi, P. & Palvadeau, P. (2000): Lead–antimony sulfosalts from Tuscany (Italy). II. Crystal structure of scainiite, Pb_{14} Sb_{30} S_{54} O_5, an expanded monoclinic derivative of Ba_{12} Bi_{24} S_{48} hexagonal sub-type (zinkenite group*). Eur. J. Mineral.* **12**, 835-846.

Mumme, W.G. (1989): The crystal structure of $Pb_{5.05}(Sb_{3.75}$ $Bi_{0.28})S_{10.72}Se_{0.28}$: boulangerite of near ideal composition. *Neues Jahrb. Mineral., Monatsh.*, 498-512.

Niizeki, W.& Buerger, M.J. (1957): The crystal structure of jamesonite, $FePb_4Sb_6S_{14}$. *Z. Kristallogr.* **109**, 161-183.

Orlandi, P., Meerschaut, A., Moëlo, Y., Palvadeau, P. & Léone, P. (2005): Lead–antimony sulfosalts from Tuscany (Italy). VIII. Rouxelite, Cu_2Hg Pb_{22} Sb_{28} S_{64} $(O, S)_2$, a new sulfosalt from Buca Della Vena mine, Apuan Alps: definition and crystal structure. *Can. Mineral.* **43**, 919-933.

Orlandi, P., Moëlo, Y., Campostrini, I. & Meerschaut, A. (2007): Lead–antimony sulfosalts from Tuscany (Italy). IX. Marrucciite, $Hg_3Pb_{16}Sb_{18}S_{46}$, a new sulfosalt from Bucca della Vena mine, Apuan Alps: definition and crystal structure. *Eur. J. Mineral.* **19**, 267-279.

Palvadeau, P., Meerschaut, A., Orlandi, P. & Moëlo, Y. (2004): Lead–antimony sulfosalts from Tuscany (Italy). VII. Crystal structure of pellouxite, $\sim(Cu,Ag)_2$ Pb_{21} Sb_{23} S_{55} Cl O, an expanded monoclinic derivative of Ba_{12} Bi_{24} S_{48} hexagonal sub-type (zinkenite group). *Eur. J. Mineral.* **16**, 845-855.

Petrova, I.V., Kaplunnik, L.N., Bortnikov, N.S., Pobedimskaya, E.A. & Belov, N.V. (1978): The crystal structure of synthetic robinsonite. *Dokl. Akad. Nauk SSSR* **241**, 88-90.

Pinto, D., Bonaccorsi, E., Balić-Žunić, T. & Makovicky, E. (2008): The crystal structure of vurroite, $Pb_{20}Sn_2(Bi,As)_{22}S_{54}Cl_6$: OD-character, polytypism, twinning and modular description. *Am. Mineral.* **93**, 713-727.

Rodier, N. (1973): Structure cristalline du sulfure mixte de thulium et de cérium $TmCeS_3$. *Bull. Soc. fr. Minéral. Cristallogr.* **96**, 350-355.

Sheldrick, G.M. (1997a): Shelxs-97. *A Computer Program for Crystal Structure Determination.* University of Göttingen, Göttingen, Germany.

Sheldrick, G.M. (1997b): Shelxl-97. *A Computer Program for Crystal Structure Refinement.* University of Göttingen, Göttingen, Germany.

Received December 11, 2007, revised manuscript accepted January 18, 2009.